Number and proportion of *P. falciparum* gametocytes vary from acute infection to chronic parasite carriage despite unaltered sexual commitment rate

Hannah van Dijk[1*], Martin Kampmann[2,3*], Nathalia F Lima[1], Michael Gabel[4], Usama Dabbas[1,2], Safiatou Doumbo[5], Hamidou Cisse[5], Shanping Li[6], Myriam Jeninga[7], Richard Thomson-Luque[1], Didier Doumtabe[5], Michaela Petter[7], Kassoum Kayentao[5], Aissata Ongoiba[5], Teun Bousema[8], Peter D Crompton[6], Boubacar Traore[5], Frederik Graw[4,9,10], Silvia Portugal[1,2±]

[1] Center for Infectious Diseases, Parasitology, Heidelberg University Hospital, Heidelberg, Germany
[2] Max Planck Institute for Infection Biology, Berlin, Germany
[3] Humboldt-Universität zu Berlin, Berlin, Germany
[4] BioQuant-Center for Quantitative Biology, Heidelberg University, Heidelberg, Germany
[5] Mali International Center of Excellence in Research, University of Sciences, Techniques and Technologies of Bamako, Mali
[6] Laboratory of Immunogenetics, National Institute of Allergy and Infectious Diseases, National Institutes of Health, Rockville, Maryland, USA
[7] Mikrobiologisches Institut-Klinische Mikrobiologie, Universitätsklinikum Erlangen
[8] Radboud University Medical Center, Nijmegen, the Netherland
[9] Interdisciplinary Center for Scientific Computing, Heidelberg University, Heidelberg, Germany
[10] Department of Internal Medicine 5, Hematology and Oncology, Friedrich-Alexander-Universität Erlangen and University Hospital Erlangen, Erlangen, Germany

[*] Equal contribution
[±] Corresponding author: portugal@mpiib-berlin.mpg.de (SP)

Abstract

Plasmodium falciparum infections persist through long dry seasons at low parasitaemia without causing malaria symptoms and thus remain untreated. In asymptomatic children, increased circulation of infected erythrocytes without adhering to the vascular endothelium is observed during the dry months, compared to febrile malaria in the wet season. However, alterations of parasite sexual commitment and gametocytogenesis have not been investigated. Here, we compared the expression of genes related to sexual commitment and gametocytogenesis, the proportion and density of *P. falciparum* gametocytes, and the blood concentration of phospholipids in dry season asymptomatic individuals versus symptomatic subjects in the wet season. Additionally, we adapted a within-host mathematical model considering asexual and sexually-committed parasites and gametocytes to understand the dynamics of gametocyte number and proportion as infections progress. Compared to clinical malaria cases, transcripts of late-stage gametocytes were predominantly upregulated in the dry season, associating with increased proportions of mature gametocytes; while transcription of genes related to parasite sexual commitment was unaltered throughout the year. Our data suggest that gametocyte density and proportion diverge as infections progress from recent transmission to chronic carriage, without alterations in the sexual commitment rate over time.

Introduction

The malaria-causing parasite *Plasmodium falciparum* requires a mosquito to complete its lifecycle and be transmitted between humans[1]. During blood-feeding, infected mosquitoes deposit sporozoites in the human dermis that can reach the circulation, arrive at the liver and infect hepatocytes, where thousands of merozoites are formed and later released into the blood stream to start continuous asexual intra-erythrocytic replication cycles of ~48h. A small proportion of asexual parasites commit to sexual development[2]. Instead of another ~48h asexual replication leading to 8-30 new merozoites ready to continue asexual cycles, the parasite develops into a sexually-committed schizont producing the same number of sexually-committed merozoites. Upon infection of new red blood cells (RBCs) each sexually-committed merozoite produces one stage I gametocyte[3,4] that in 8-12 days goes through five developmental stages[5]. Stages II-IV of gametocyte development occur in the bone marrow or spleen[6,7], and therefore do not circulate; while stage V gametocytes circulate up to ~20 days[8,9], waiting for another mosquito-bite. In the mosquito midgut, gametocytes transform into female and male gametes that fuse into a zygote, which develops into an ookinete. In the midgut wall, the ookinete generates sporozoites that reach the mosquito salivary glands and can restart the lifecycle. Continuous presence of mosquitoes and humans allows perennial malaria transmission. However, in areas with months-long dry season, the mosquito population plummets to zero[10], transmission is interrupted and *P. falciparum* survives in humans until mosquitos return in the ensuing wet season[11-13]. Long mosquito-free periods make gametocyte production a dead-end since these cannot survive to bridge two wet seasons[8,9]. Dynamically adapting sexual commitment rates depending on transmission environment, e.g. through sensing of dry-season associated cues, would represent a benefit for the parasite, as waste of resources could be avoided. Whether the parasite dynamically alters resources allocation into transmission to the mosquito to adapt to environmental changes remains unclear. Various factors such as host age[14], haematocrit[15], haemoglobin type[16] and duration of symptoms[17] have been linked to gametocytaemia in individuals with clinical malaria. Higher frequencies of gametocyte-positive individuals were observed in chronic asymptomatic infections compared to acute infections[18-22]. In vitro conditions have been shown to directly influence sexual commitment and gametocytogenesis[3,23-25]. Lysophosphatidylcholine (Lyso-PC) has been identified as repressor of the pro-sexual commitment transcription factor AP2G, and low levels of Lyso-PC have been found to increase the proportion of sexual forms in vitro[25]. Gametocyte development protein 1 (GDV1) was described as the de-repressing effector, which promotes *ap2g* expression and induces gametocytogenesis[26], and homeodomain protein 1 (HDP1) acts as a positive regulator of gametocyte development[27]. A shift in intracellular S-adenosylmethionine/S-adenosyl homocysteine has been shown to affect histone methylation and increase parasites commitment to sexual differentiation[28]. Still, it remains unclear how sexual commitment rates are regulated in vivo and whether the parasite can optimize its transmission-investment. A study on controlled human

malaria infections investigated whether mosquito bites, a plausible seasonal cue, could induce gametocytogenesis found no evidence of such an effect [29].

Dry season *P. falciparum* parasites exhibit a transcription pattern distinct of that of parasites causing febrile malaria during the wet season[11,30]. These seasonal transcriptional differences reflect longer parasite circulation within each ~48h intra-erythrocytic cycle in the dry season, leading to increased splenic clearance of iRBCs and contributing to the low parasitaemias observed during the dry season[11], but alterations of parasite sexual commitment and gametocytogenesis remain unexplored.

Here, we compared sexual commitment and gametocytogenesis of parasites persisting through the dry season with those of parasites in clinical malaria cases. We found that clinical malaria cases consistently exhibit higher parasite densities compared to asymptomatic infections, and that expression of marker genes of mature gametocytes and the proportion of gametocytes among all parasites were higher in persisting infections; while sexual commitment did not substantially vary longitudinally within each individual. Additionally, we determined that serological differences observed throughout the year were unable to differently induce *P. falciparum* gametocytogenesis in vitro. Finally, adapting a previously described within-host mathematical model[31], we inferred the dynamics of gametocyte number and proportion as infections progress from recently transmitted through chronic asymptomatic dry season carriage. We conclude that a constant sexual commitment rate allows for dynamic alterations of sexual stages of *P. falciparum* consistent with empirical observations.

RESULTS

Seasonal transcriptional patterns of *P. falciparum* sexual development, and lipid concentration in plasma.

Previously, we described transcriptional differences between *P. falciparum* from asymptomatic children at the end of the dry season and children with clinical malaria in the wet season[11]. Now, we extend our analysis to focus on sexual development across the two conditions and started by compiling a list of genes related to gametocytogenesis from four RNAseq published studies to query potential adaptations of *P. falciparum* sexual stages to asymptomatic persistence (Supplementary Table 1). Painter et al. reported 786 gametocyte-related transcripts in vitro[32], of which we detected 333 in the dry vs wet season dataset[11]. Poran et al. described early and late gametocyte transcripts comparing day 2 vs 9 of gametocytogenesis[33], we found that 2 out of 3 early gametocyte transcripts and 15 out of 17 late-gametocyte transcripts were detected in the dry vs wet season dataset. Lopez-Barragan et al. compared days 4 vs 15 of gametocytogenesis and identified 41 early- and 58 late-gametocyte genes[34]. Of those, 32 and 44 were detected in the dry vs wet season dataset[11]. Finally, Jeninga et al.[35] compared days 4 vs 10 of gametocytogenesis

117 and identified 237 transcripts assigned to early-gametocytes independent of sex, as well as 314
118 late gametocyte genes. Out of these, 80 early- and 133 late-gametocyte genes were detected at
119 the end of dry vs wet season dataset[11]. The full list of 1258 sexual commitment- and
120 gametocytogenesis-related genes showed limited overlap between reports (Supplementary Table
121 1), potentially due to the different timepoints and comparison conditions defined in the different
122 studies. In summary, in the end of dry season asymptomatic vs wet season clinical cases RNAseq
123 dataset[11] we detected 551 of the 1258 genes, which could be expressed in circulating sexually-
124 committed asexual stages, stage I or stage V gametocytes. Principal component analysis of
125 expression values of these 551 genes expressed in *P. falciparum* of asymptomatic children at the
126 end of the dry season and children with clinical malaria in the wet season[11] revealed segregation of
127 transcription profiles based on seasonality and clinical presentation (Fig. 1A), and clustering by
128 similarity also produced visible seasonal patterns (Supplementary Fig. 1). We performed gene set
129 enrichment analysis (GSEA) to assess whether gametocyte-associated genes (described by
130 López-Barragán et al., Jeninga et al., Poran et al., and Painter et al.), were modulated in dry
131 season infections. Genes from each study were analyzed separately, and López-Barragán et al.
132 and Jeninga et al. also allowed distinguishing between early- and late-stage gametocytes.
133 Furthermore, we combined all early- and all late-stage defining genes into early and late
134 gametocyte supersets. Due to the small number of genes reported by Poran et al., these data were
135 not individually analyzed but incorporated into the all early and all late supersets. We identified
136 statistically significant enrichment of the Jeninga et al. late-gametocyte gene set (normalized
137 enrichment score, NES=1.29, p-value=4.053*10^-3), the López-Barragan et al. late-gametocyte
138 gene set, (NES=1.76, p-value=9.235*10^-9), as well as the late gametocyte superset (NES=1.49,
139 p-value=3.11*10^-7), and the Painter et al. gene set of gametocyte-associated genes (NES=1.42,
140 p-value=5.01*10^-6) among genes up-regulated at the end of the dry season vs wet season clinical
141 malaria cases, while none of the early-gametocyte gene sets afforded statistically significant
142 enrichment (Fig. 1B). Accordingly, we observed a higher proportion of the late-gametocyte specific
143 transcripts upregulated in the end of dry season asymptomatic vs wet season clinical cases
144 RNAseq dataset[11] (Supplementary Table 1) compared to the proportion of early-gametocyte
145 specific transcripts. Close to two thirds (65%) of late-gametocyte transcripts were upregulated in
146 the dry season (112/172 genes, Chi^2 *p*-value < 0.00001), while only 39% (43/109 genes, Chi^2 *p*-
147 value=0.36784) of early-gametocyte transcripts, and 33% of total *P. falciparum* transcripts
148 (1131/3381 genes) were upregulated at the end of the dry season in May (Fig. 1C). Markers of
149 female (*pfs25*, PF3D7_1031000) and male (*pfmget*, Pf3D7_1469900) late-stage gametocytes were
150 among the upregulated transcripts at the end of the dry season, in May, in the same RNAseq
151 dataset[11] (Supplementary Table 1).

152 These transcriptional differences prompted us to quantify the relative expression of female and
153 male gametocyte-coding genes in 68 samples (MAL n=31, May n= 37) collected from the same
154 cohort study as the reported RNAseq data[11], from asymptomatically infected children at the end of
155 the dry season (May) and age and sex-matched children presenting with clinical malaria symptoms
156 in the wet season (MAL). qRT-PCR of marker genes of female (*pfs25*, PF3D7_1031000) and male
157 (*pfmget*, Pf3D7_1469900) gametocytes relative to a housekeeping gene (*glycine-tRNA ligase*,
158 PF3D7_1420400) confirmed the increased expression of the female gametocyte associated gene
159 in May at the ebd of the dry season, compared to malaria cases (Fig. 1D). Conversely, transcripts
160 known to regulate sexual commitment (*ap2g*, PF3D7_1222600; and *gdv1*, PF3D7_0935400), and
161 transcripts expressed by sexually-committed schizonts (*msrp1*, PF3D7_1335000), or by early-
162 gametocytes (*gexp5*, PF3D7_0936600) did not appear differentially expressed in the end of dry
163 season asymptomatic vs wet season malaria cases RNAseq dataset[11] (Supplementary Table 1).
164 qRT-PCR analysis of the regulator of sexual commitment, *ap2g*, and the early gametocyte marker
165 *gexp5* confirmed the absence of significant differences between the conditions (Fig. 1E). We then
166 performed shotgun lipidomics with 40 samples from the same study site to examine potential
167 associations between gametocyte proportion and plasma Lyso-PC and
168 lysophosphatidylethanolamine (Lyso-PE) composition. The lower expression of late-gametocyte
169 genes in the 20 malaria cases (MAL) coincided with lower levels of several species of the Lyso-PC
170 and Lyso-PE families compared to the 20 asymptomatic carriers at end of the dry season (May)
171 (Fig. 1F), suggesting that LysoPC levels might not be responsible for the observed gene
172 expression changes, but rather a consequence of high parasitaemias and inflammation during
173 acute infection.
174 Additionally, we interrogated whether the low phospholipids levels in plasma of malaria cases in
175 the wet season compared to dry season persistent dry season infections in May, could sexual
176 conversion and result in different gametocytaemia in vitro. We exposed *P. falciparum* of the Pf2004
177 strain to plasma collected from 19 clinical malaria patients in the wet season (MAL) or from 18
178 asymptomatically infected children at the end of the dry season (May), alongside the previously
179 described conditions[25] to induce or inhibit sexual conversion and gametocyteamia. As reported[25],
180 we observed that 24h after culture without serum (-S), and thus without Lyso-PC, sexual
181 conversion rate increased compared to parasites cultured in the presence of 10% serum (+S) or
182 without serum but supplemented with 20 μM Lyso-PC (LPC) (Fig. 1G). However, conversion rates
183 into gametocytes five days after treatment did not show a statistically significant difference between
184 supplementation with 25% of plasma from children with clinical malaria (MAL), plasma from dry
185 season asymptomatic carriers (May), or German pooled plasma (German) (Fig. 1G). The induced
186 sexual commitment rates were variable and did not associate to disease status or season of the
187 tested plasma, indicating that the differences in Lyso-PC between asymptomatic children and

malaria cases (Fig. 1F) were insufficient to impose alterations in sexual commitment or gametocytaemia.

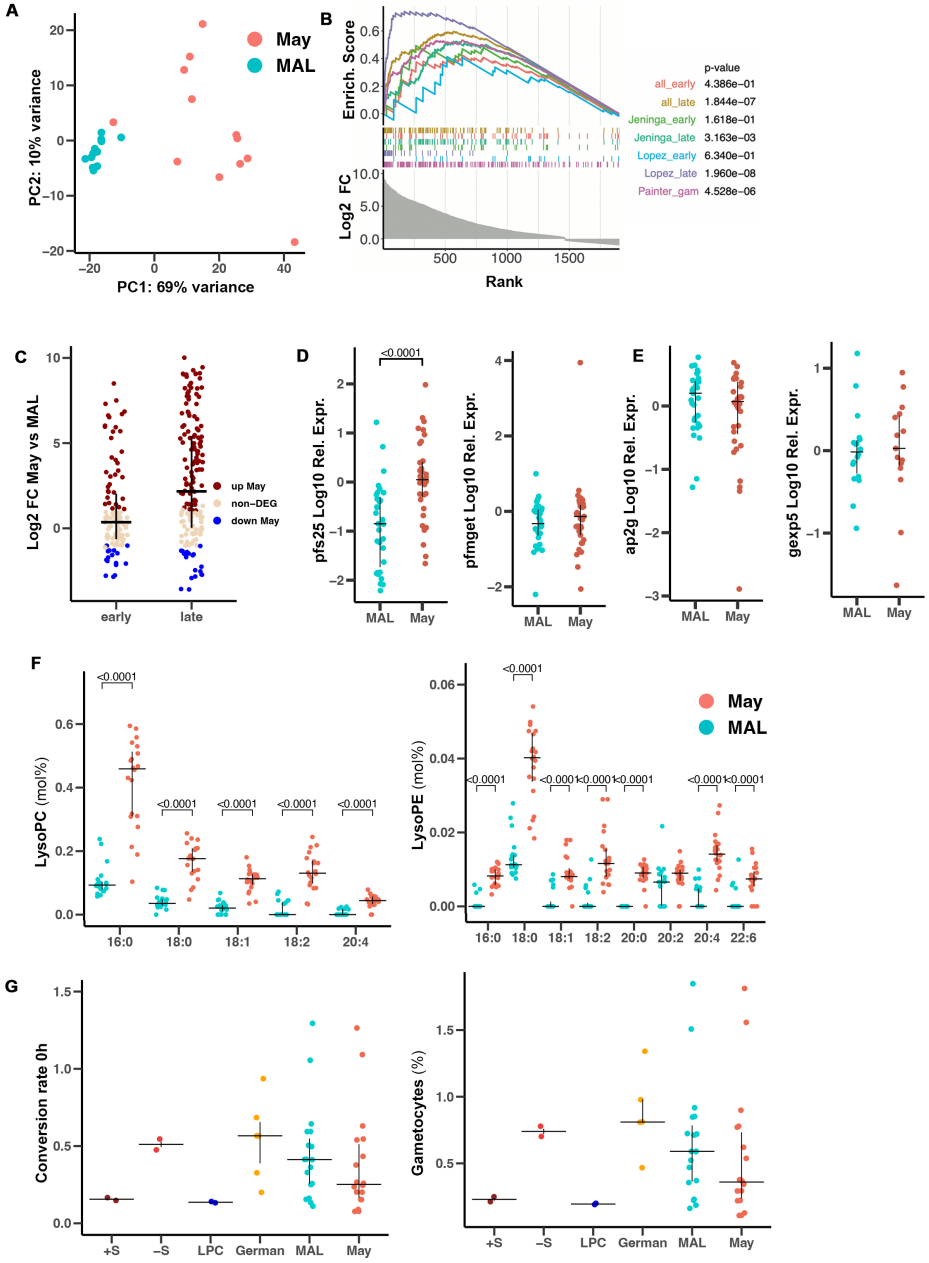

Figure 1. *P. falciparum* transcription and gametocytogenesis in clinical malaria and at the end of the dry season. A Principal components analysis of RNA-Seq data of 551 transcripts gametocyte specific *P. falciparum* genes from parasites collected at the end of the dry season and from clinical malaria cases (n= 12 May, 12 MAL). **B** Gene set enrichment analysis of gametocyte associated gene published by López-Barragán et al.; Jeninga et al., Painter et al. among DEGs between parasites collected at the end of the dry season (n=12) and from clinical malaria cases (n=12). All_early and All_late sets are collated from Lopez-Barragan et al., and Jeninga et al. and gametocyte associated genes published in Poran et al.. DEGs identified between clinical malaria cases and dry season asymptomatic infections were ranked by log2fold-change and GSEA-analysis performed with the fgsea algorithm. **C** Fold change of early and late gametocyte transcripts between parasites collected at the end of the dry season and from clinical malaria cases (n= 12 May, 12 MAL) according to López-Barragán et al.; Poran et al., and Jeninga et al.. Each dot represents a gene and color identifies fold change direction. **D** Relative expression of markers of female (*pfs25*, left) and male gametocytes (*pfmget*, right) to a housekeeping gene (*glycine-tRNA-ligase*)

detected by qRT-PCR in clinical malaria cases (MAL, n=31) and in RDT$^+$ subclinical children at the end of the dry season (May, n= 37). **E** Relative expression of *ap2g* and *gexp5* detected by qRT-PCR in clinical malaria cases and in RDT$^+$ subclinical children at the end of the dry season. (MAL n=31, and May n=37 for *ap2g* and MAL n=18, and May n=15 for *gexp5*). **F** Plasma concentration of Lyso-PC (left) and Lyso-PE (right) species in RDT+ subclinical children at the end of the dry season (May, n=20) and in children with their first clinical malaria episode (MAL, n=20) in the wet season. **G** Pf2004 conversion rate (gametocytes d5/parasites d2) (left) and gametocyte density (right) detected by microscopy, after 24h culture with 25% plasma collected during clinical malaria episodes in the wet season (MAL n=19) or at the end of the dry season (May n=18), or German pooled plasma (German) alongside without serum (-S), serum supplemented (+S) and Lyso-PC supplemented (LPC) conditions. Lipid data and expression values represented as median ± IQR; Wilcoxon test between MAL and May with Bonferroni multiple comparison correction. Conversion rates represented as median ± IQR; Wilcoxon test.

Sexual commitment and gametocytogenesis dynamic in persisting infections

Next, we obtained plasma and parasite samples collected longitudinally throughout the dry and wet seasons in the same cohort study, to investigated associations between expression of gametocyte-related genes and plasma Lyso-PC in children continuously infected from the wet until the end of the dry season, and in children with clinical malaria cases in the wet season. Within previously reported metabolomic data of this cohort [36], we found that Lyso-PC 18:0 was lower in clinical malaria cases (MAL n=15) compared to asymptomatic infections from different timepoints (Oct n=17, Mar n=19, and May n=19); and it also decreased from the wet (Oct) to the end of the dry season (May) (Fig. 2A). Lyso-PC 18:0 levels in persistent infections (Oct, Mar and May) were comparable to those in non-infected individuals at the end of the dry season (May$^-$), indicating little or no impact of asymptomatic infections on Lyso-PC 18:0 (Fig. 2A).

We then sought to relate these data with gene expression of gametocyte-related genes at different timepoints along the year, we used qRT-PCR of female, and male gametocyte markers relative to a housekeeping gene. Our results confirmed that the relative expression of female and male gametocytes markers, although variable, was significantly higher at any timepoint of asymptomatic infection (Oct n =14, Jan n=17, Mar n=17, and May n=18) than in clinical cases of malaria (MAL, n=19) (Fig. 2B). In contrast, no differences were found between the timepoints of asymptomatic infection (Oct, Jan, Mar and May) (Fig. 2B). The expression of *ap2g* was not significantly different across seasons or clinical presentations (Fig. 2B). In addition, no significant correlations were detected between the concentration of LysoPC 18:0 and the expression of *pfs25* (Spearman's cor 0.286, p-value=0.1474), *pfmget* (Spearman's cor 0.359, p-value=0.0934) or *ap2G* (Spearman's cor -0.082, p-value=0.7372) (Fig. 2C), though we did observe a trend of lower LysoPC 18:0 concentrations in clinical malaria cases, that also showed reduced *pfs25* and *pfmget* expression.

Figure 2. Plasma concentration of LysoPC and its effect on sexual commitment in persistent and clinical infections. A Plasma concentration of Lyso-PC 18:0 during clinical malaria episodes (MAL n=15), RDT^{+} subclinical infection times during the wet (Oct n=17) and the dry season (Mar and May n=19), and of uninfected children at the end of the dry season (May- n=20). **B** Relative expression of markers of female gametocytes (*pfs25*, left), male gametocytes (*pfmget*, centre), and sexual commitment (*ap2g*, right) relative to a housekeeping gene (Gly-tRNA-ligase)detected by qRT-PCR of RDT^{+} subclinical children at different times during the wet (Oct n=14) and the dry season (Jan n=17, Mar n=17, May n=18), and during clinical malaria episodes (MAL n=19). **C** Spearman correlation between Lyso-PC 18:0 and the relative expression of markers of female gametocytes (*pfs25*, left), male gametocyte (*pfmget*, centre), and parasite sexual commitment (*ap2g*, right) . Lipid data and rel expr values compared by Dunn's Kruskal-Wallis test with Bonferroni multiple comparison correction. Paired samples of the same individuals are connected on plots.

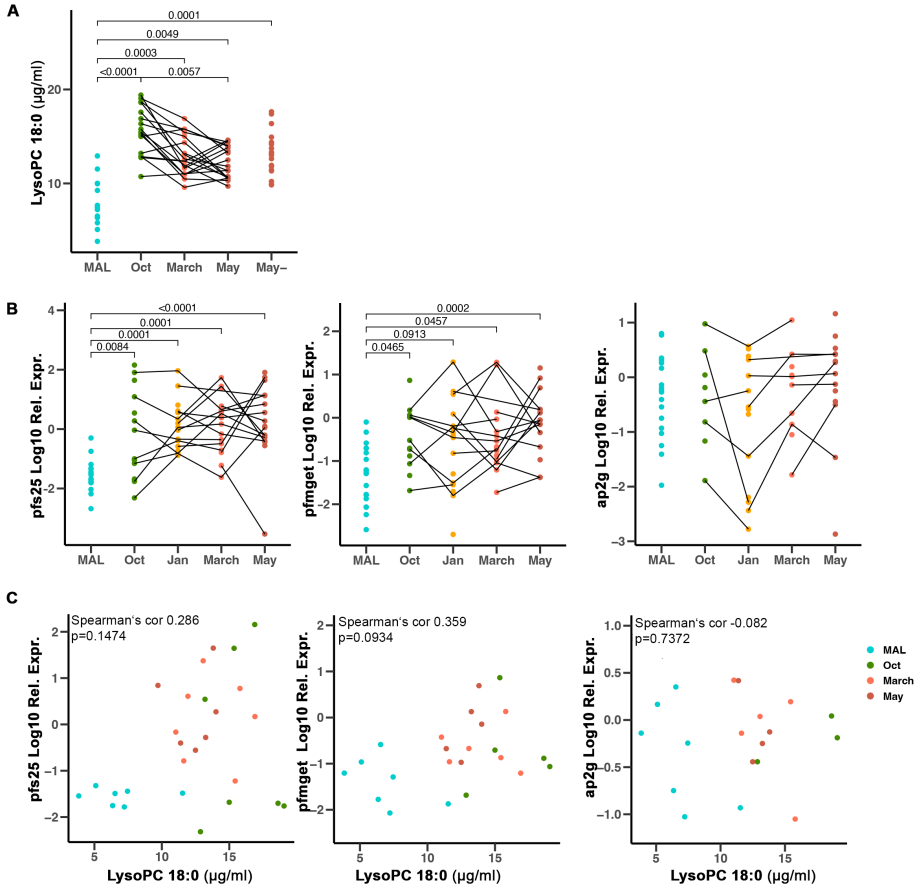

Higher gametocytes proportion in asymptomatic vs clinical infections is independent of seasonality

We then investigated how density and proportion of gametocytes differed between clinical malaria and asymptomatic infections in settings with different seasonality patterns. While Mali experiences contrasting seasons with 5-6 months interruption of transmission every year[10], Uganda has uninterrupted year-round transmission peaking at times of strong rain[37]. To quantify parasites and female gametocytes in Malian samples as well as proportion of gametocytes out of all iRBCs, we prepared standard curves of asexual parasites and sorted sex-specific fluorescent gametocytes[38] (Supplementary Fig. 2). Then, we quantified expression of *glycine-tRNA-ligase* and *pfs25* in 19

266 clinical malaria cases and 50 paired samples (Jan n=25, May n=25) collected from asymptomatic
267 infected individuals at the beginning and end of the dry season, and determined parasitaemia and
268 gametocytemia based on these curves.
269 To investigate parasite and gametocyte carriage in a non-seasonal setting in Uganda, we obtained
270 total parasite and female gametocyte densities previously published[37] and retrieved from
271 ClinEpiDB[39]. This analysis included qRT-PCR quantifications of *ccp4* (PF3D7_0903800) and the
272 multilocus *varATS* of 150 individuals with asymptomatic parasitaemias persisting for over one
273 month (n=122) and age-matched individuals with clinical malaria (n=38). In Uganda, we detected
274 93% of gametocyte prevalence in asymptomatic infections (n=114) and 34% in clinical cases
275 (n=13). In Mali, the prevalence of gametocytes was 69% in the beginning of the dry season in Jan
276 (n=18), and 76% at the end of the dry season in May (n=19) with 11 individuals being positive at
277 both timepoints. Prevalence of gametocytes in clinical cases presented was 89% (n=17). We found
278 significantly higher asexual parasite levels among gametocyte positive samples in clinical malaria
279 cases compared to asymptomatic infections in both settings (Fig. 3A). In addition, a significantly
280 higher density of gametocytes in clinical compared to asymptomatic infections in the Uganda
281 setting was observed, while the difference in Mali was not statistically significant (Fig. 3B).
282 Furthermore, we observed a lower density but higher prevalence of gametocytes (89%) in Malian
283 clinical cases compared to Ugandan clinical samples (34%), suggestion differences in
284 experimental procedure between the two studies might account for the discrepancy in
285 gametocytaemia, with low gametocytaemia in clinical samples remaining undetected in malaria
286 cases of the Ugandan cohort (Fig. 3B). Next, we aimed to determine the proportion of gametocytes
287 of the total parasite population in both settings. Our data showed that in both Mali and Uganda,
288 gametocytes constitute a larger proportion of the total parasite population in asymptomatic
289 infections than in clinical cases of malaria (Fig. 3C), in line with the described increased relative
290 expression of gametocyte-marker genes (Fig. 1 and 2). On the other hand, transcription of *ap2g*
291 was comparable in the Malian clinical and asymptomatic samples (Fig. 3D). Also in the Malian
292 setting, paired samples from the beginning and end of the dry season revealed a significant
293 decrease of parasite load from January to May (Fig. 3E), while no significant difference in
294 gametocyte levels (Fig. 3F), or commitment rate measured by *ap2G* expression were detected
295 (Fig. 3G), supporting unaltered sexual commitment or gametocyte development throughout the dry
296 season.
297
298 **Figure 3. Proportion of gametocytes is higher in asymptomatic infections than in clinical cases. A** Parasite
299 density detected by qRT-PCR of *Glycine-tRNA-ligase*, using a standard curve of Pf2004 parasites and sorted
300 female gametocytes, in gametocyte positive symptomatic (n=13, MAL) and asymptomatic infections (n=113) in
301 Uganda; and clinical malaria cases (MAL n=17), and asymptomatic infections (Jan n=18, May n=19) from the
302 beginning and end of the dry season in Mali. **B** Gametocyte density in the same samples quantified by qRT-PCR of
303 *pfs25* relative to a standard curve of sorted female gametocytes. Samples from Uganda and Mali were compared
304 separately. p-values for the MAL-Jan comparison and Jan prevalence in Mali samples are shown in red, MAL-May
305 comparison shown in black. Values are plotted with median and IQR Dunn's Kruskall-Wallis test with Bonferroni

306 multiple comparison correction. **C** Ratio of gametocytes to asexual parasite load. Values are plotted with median
307 and IQR, Dunn's Kruskall-Wallis test, samples from Uganda and Mali were compared separately. P-values for the
308 MAL-Jan comparison are shown in red, MAL-May comparison in black **C** Relative expression of *ap2g* in malaria
309 cases (n=19) and asymptomatic dry season (Jan n= 20, May n=18) from the same sample set, Dunn's Kruskall-
310 Wallis test. **D** Parasite density, quantified by Glycine-tRNA qRT-PCR relative to a standard curve for 25 paired
311 samples from the beginning (Jan) to end of the dry season (May). Wilcoxon matched-pairs signed rank test. **E**
312 Gametocyte density quantified by *pfs25* qRT-PCR relative to a standard curve in samples from the beginning (Jan,
313 n=18) to end of the dry season (May, n=19). Wilcoxon matched-pairs signed rank test performed on 11 paired
314 samples with detectable gametocytes in both timepoints. **F** *ap2g* expression by qRT-PCR of samples from the
315 beginning (Jan, n=20) to end of the dry season (May, n=18). Wilcoxon matched-pairs signed rank test performed on
316 18 paired samples with detectable *ap2G* expression at both timepoints.

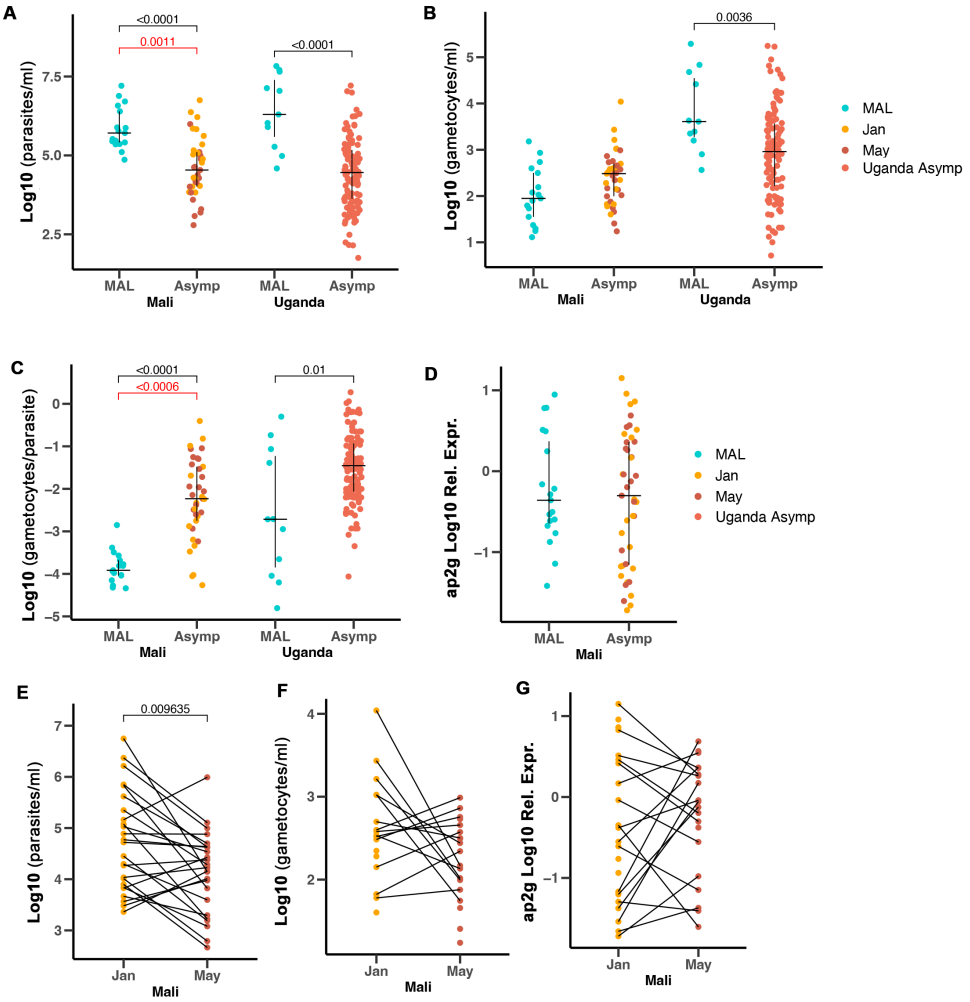

317
318

319 **Progressing infection leads to apparent differences in gametocytogenesis.**

320 We observed higher proportions of gametocytes in asymptomatic vs clinical malaria, without
321 concomitant differences in the expression of markers of sexual commitment and early
322 gametocytes. As infection progression over the course of the dry season, we observe a decrease
323 in parasitaemia, though no apparent change in the proportion of gametocytes. To explain this, we
324 devised a mathematical model considering three different parasite populations - asexual parasites
325 (P), sexually-committed parasites (PG) and gametocytes (G), all of which circulate or are

326 cytoadherent[31] (Fig. 4A). To improve the fit of an earlier model by Cao et al.[31] to our data, we
327 extended the model by incorporating the assumption of increased clearance of longer-circulating
328 iRBCs in persisting parasitaemias compared to recently transmitted parasites as reported
329 previously[11]. This distinguished two phases of infection, in which the growth of parasites varied due
330 to immune response or the parasite's adhesion properties, in agreement with reported data[37]. In
331 our model, parasitaemia increased rapidly at early timepoints after parasite egress from the liver
332 (day 0), up to day 14 when, in our model, infections transition to the chronic phase. Faster
333 clearance in the chronic phase due to immunity or splenic removal of parasites was implemented
334 as an increase in the asexual parasite removal at the transition from acute to chronic infection on
335 day 14. We then followed chronic infections up to day 180, mirroring the 6-month dry season length
336 in Mali. We fit the model to the symptomatic and asymptomatic parasitaemia and gametocytaemia
337 levels of the Malian cohort reported in Figure 3, assuming that clinical cases occur shortly after
338 transmission of parasites on day 14 of blood stage as evidenced by epidemiological studies
339 associating disease with recent transmission[12,40,41]. Asymptomatic infections at the beginning of the
340 dry season, i.e. January, were used to describe early asymptomatic timepoints (day 28), and the
341 end of the dry season in May was used as a late asymptomatic timepoint (day 180) (Fig. 4C and
342 D). Using an iterative Bayesian fitting-approach to fit the model to the symptomatic and
343 asymptomatic parasitaemia and gametocytaemia levels of the Malian cohort, we quantitatively
344 assessed biological parameters including sexual commitment rate, gametocyte circulation time,
345 and gametocyte sequestration time, confirming previously determined parameter ranges[31,42]
346 (Supplementary Table 4 and Fig. 4E). Our adapted model provided a dynamic depiction of
347 parasitaemia levels, as well as gametocyte densities and proportions, as seen in the Malian data.
348 In line with our data and previous literature [43], parasitaemia in chronic infection decreased following
349 a log-linear pattern until day 180 (Fig. 4B).
350 Maintaining the fraction of parasites entering sexual commitment, *f*, constant throughout acute and
351 chronic infection phases, our model predicted a lower proportion of gametocytes in the acute
352 phase (Fig. 4D), when parasitaemia increased rapidly. Due to the maturation time of gametocytes
353 outside of circulation, gametocytemia lags behind parasitaemia, as gametocyte levels are reflective
354 of parasite density at the time when sexual commitment occurred. This trend is reversed during the
355 chronic phase of infection due to the negative growth of asexual parasites imposed by increased
356 removal of iRBCs. After a transition phase when the proportion of gametocytes in the population
357 increased, the gametocyte proportion reached a higher equilibrium (Fig. 4D). Therefore, a model
358 with a fixed commitment rate seemed capable of reproducing the patterns of parasitaemia and
359 gametocytaemia as we observed in the Malian data.
360 To further test how alternative assumptions would affect data explainability, we investigated how a
361 dynamic commitment rate would influence parasite and gametocyte dynamics as infection

progresses. To this end, we modified the model framework to investigate two additional scenarios, in which the commitment rate changes as infection progresses. Scenario 2 assumes that the sexual commitment changes during the persistent phase of infection, i.e. at day 100 post infection, reflecting potential changes due to seasonal cues (Supplementary Fig. 3A). In contrast, scenario 3 allows for a varying commitment at the time of peak parasitaemia, i.e. between day 7 and 21, mimicking the potential impact of Lyso-PC depletion in the blood stream (Supplementary Fig. 3B). Using the same Bayesian fitting-approach, we fitted the two alternative models to the data and compared their descriptive power (Supplementary Fig. 4A) and inferred parameter ranges (Supplementary Fig. 3C). Our original (scenario 1) and scenarios 2 and 3 were able to explain the observed dynamics with similar posterior distributions for all model parameters other than the commitment rates (Supplementary Table 4, Supplementary Fig. 5A).

Commitment rates in scenario 1, 2 and 3 fell in a similar range. Although in scenario 2 and 3 the range of estimated commitment rates in the persistent phase of infection were wider and also showed tendencies towards higher estimates if algorithms were run for longer, they still overlapped with the constant commitment rate assumed in scenario 1 with differences of the commitment rates between different scenarios remaining minor in absolute terms. Thus, the data do not contain enough support for a scenario that assumes a changing commitment rate, as a fixed commitment rate is equally likely to provide a dynamic depiction of the observed gametocyte densities and proportions and is generally preferred by the model selection criteria (Supplemental Figure 5).

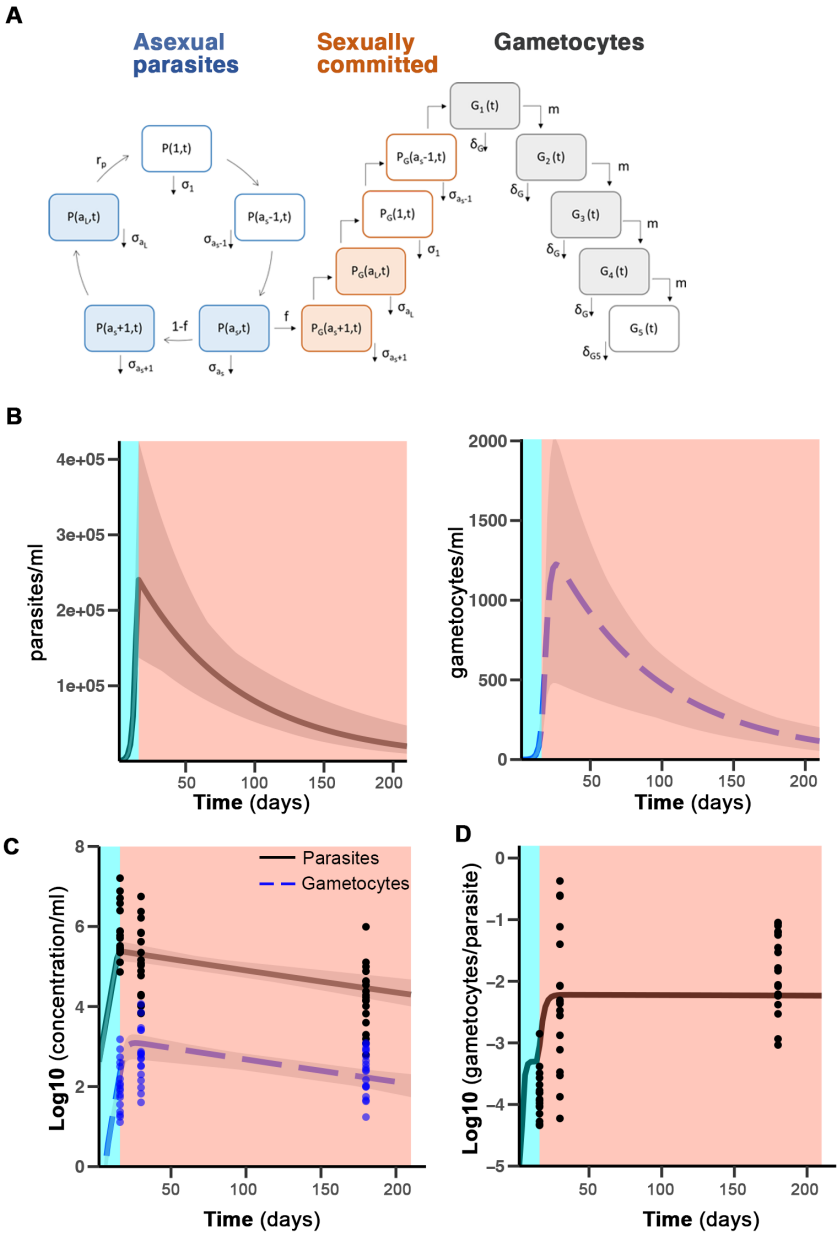

E

	Scenario 1	
Sexual Commitment Rate	0.11- 0.404 %	
Modified Sex. Commitment Rate	NA	
Gametocyte Circulation time	1.9 - 2.4 days	
Gametocyte Sequestration time	3.1 - 4.8 days	
	Acute Phase	Chronic Phase
Parasite multiplication factor	2.39 - 3.02	0.76 - 1.22

Figure 4. **A** Sketch of the mathematical model to describe parasite dynamics including individual compartments, transitions and death rates: Asexual parasites (P) replicate in a 48h cycle, being cleared at an age dependent death rate (σ_a). A fraction of asexual parasites (f) transitions to the sexually committed parasite compartment (PG), goes through a round of replication and develops into gametocytes (G). Gametocytes mature over 5 distinct stages. Asexual parasites (blue), sexually committed parasites (orange) and gametocytes (grey). **B** Model prediction of development of parasitemia (left) and gametocytemia (right) with infection progression. Parasitemia and gametocytemia were averaged over one replication cycle (48h). Solid and dashed lines show average of model predictions based on posterior parameter distribution, with grey shaded areas corresponding to the range of model predictions. **C** Parasitemia and gametocytemia. Lines indicate model prediction, points refer to the actual measurements of gametocytemia for MAL (d14), Jan (d28) and May (d180). **D** Ratio of gametocytes/parasites as predicted by the model (lines) and individual measurements for clinical malaria cases (d14), Jan (d28) and May (d180). **E** Parameter estimates in distinct phases of *P. falciparum* infection shown as 89% credibility interval of the posterior distributions. The sexual commitment rate defined by the fraction of parasites that are sexually committed, *f*, is given in %.

450 **Discussion**

451 The absence of mosquitoes during dry months and the limited lifespan of *P. falciparum*
452 gametocytes[8,9] renders the production of gametocytes useless during the dry season. However,
453 gametocytes must be available to resume malaria transmission when mosquitos return each wet
454 season. Whether *P. falciparum* maintains a constant rate of producing sexual forms or adjusts
455 gametocytogenesis to optimize transmission and fitness is unclear. In this study, we used samples
456 from Malians exposed to alternating six-month dry and wet seasons, as well as samples from
457 clinical malaria and persisting *P. falciparum* infections from Uganda, where transmission occurs
458 year-round. Our findings demonstrate that clinical malaria cases show higher parasite and similar
459 or higher stage V gametocyte densities compared to asymptomatic infections. However, the
460 proportion of gametocytes is increased in asymptomatic persisting infections. Additionally, we
461 observed that transcription of genes characterizing sexually-committed parasites and stage I
462 gametocytes[44,45] were unaffected by season or symptoms. This clearly contrasts with genes of
463 late-gametocytes, which were enriched among upregulated transcripts in persisting infections at
464 the end of the dry season. Together these observations suggest that gametocytogenesis remains
465 constant as infections progress from recent transmission to chronic carriage, and it is the difference
466 in asexual survival/replication rates that promotes different gametocyte levels.

467 It has been suggested that *P. falciparum*'s investment in gametocyte production adjusts to host
468 nutrient availability[46], drug pressure[17], transmission intensity[47], host inflammatory state[48], and
469 seasonality[49,50], but results are inconsistent and potentially affected by the dynamics of asexual
470 parasite growth. In Sudan, it was observed that gametocyte density increased prior to the highest
471 transmission peak[51], suggesting higher gametocyte investment. In Burkina Faso, gametocyte
472 densities were higher at the peak and end of the transmission season than during the dry
473 season[52], while the efficiency of mosquito infection through membrane feeding was greater early in
474 the transmission season than at the peak of the wet or the dry seasons[53]. Nevertheless, these
475 studies did not monitor the same parasite population longitudinally from the dry into the wet
476 season. Also, in Burkina Faso, transmission was more effective in persistent than in incident
477 infections, but data collection ended after day 35, and all collections were done during the wet
478 season[18].

479 In vitro studies have shown that depleting Lyso-PC or choline induce *ap2G* expression and
480 increased gametocyte production[25,54], but associations in vivo are less consistent. In Rwanda, low
481 Lyso-PC levels were associated with higher parasite densities[55], while in Ghana, although
482 correlations with parasitaemia were not reported, Lyso-PC levels inconsistently associated with
483 gametocyte-committed rings converting into gametocytes in vitro[45]. Our data, similar to Orikiiriza et
484 al.[55], demonstrate an association between lower Lyso-PC levels and increased parasitaemia and
485 malaria symptoms. However, this association was lost at low parasitaemias, and Lyso-PC levels

were unaffected by asymptomatic carriage compared to non-infected individuals. In line with previous reports of parasitaemia affecting lipid levels by its consumption for parasite growth[25]. In vitro, drugs also affect sexual conversion; sub-curative doses of dihydroartemisinin (DHA) stimulate *ap2g* expression and sexual conversion of trophozoite-, but not ring-stages. But this increase could not synergize with choline depletion, suggesting that the effects of DHA on lipids, might be the same as choline depletion[54,56]. In vivo, it has been shown that after artemisinin treatment, *ap2g* expression increases in many, but not all patients, and data varied significantly between cohorts. These findings highlight the complex regulation of sexual conversion which is influenced by patient, parasite characteristics[57], and resistance status[58]. Our RNA-seq and RT-qPCR data reveal a constant expression of *ap2g* and unaltered expression of transcripts associated with committed schizonts and early-gametocytes, suggesting that reduced Lyso-PC observed during uncomplicated clinical malaria is unable to affect *P. falciparum* sexual commitment. Accordingly, in vitro supplementation with plasma from clinical malaria cases or end of the dry season infected individuals did not differentially affect the parasite's sexual conversion rate. This supports that Lyso-PC differences introduced by *P. falciparum* infection are not sufficient to trigger the mechanisms demonstrated in vitro[25,54]. Nevertheless, it is possible that in specific niches Lyso-PC levels are sufficiently low to trigger the sexual commitment of parasites, although this requires the presence of iRBCs in such niches to respond to the stimulus.

Previous studies on gametocytogenesis did not consider the dynamic changes within the asexual compartment during persistent infections. Greischar et al. demonstrated the difficulty of quantifying transmission investment by comparing existing quantification methods on simulated data with known transmission investment[59], while Prajapati and colleagues relied on in vitro culture of sexually committed circulating parasites to define samples with varying commitment rates[60]. Also, our study has limitations; the quantification of parasite and gametocyte densities may be affected by primer efficiencies, which may impact comparisons across different transcript measurements, although our relative analysis to a standard curve minimizes such effects. Although we lack longitudinal data and make assumptions about the timing of clinical and asymptomatic infections during infections progression, and while our model only represents the dynamics of infections with a single parasite strain, our model can explain the observed patterns by assuming transitions from a faster to a slower asexual growth rate[61]. Despite these limitations, we show that the proportion of sexual stages is inversely related in recent transmissions versus chronic infections, without alteration in the expression of regulators of sexual commitment while maintaining a constant rate of sexual commitment. Taking into account that persisting infections beyond the acute immune response exhibit prolonged circulation and increased splenic clearance[11], allowed us to complement the model by Cao et al.[31] with an increased asexual parasite death rate following the immuno-responsive period based on reports of prolonged circulation and increased splenic

522 clearance[11]. This promotes a progressive increase in the representation of sexual stages in later
523 phases of infection, which recent data showing peak of gametocyte density preceding by several
524 weeks the peak of gametocyte proportions, also support[22]. The low gametocyte proportions early in
525 infection are due to the lag of ~8-12 days of gametocyte development in the bone marrow, while
526 asexual replication efficiently increases in the absence of adaptive immunity. Data of controlled
527 infections has indeed shown that parasitaemia is predictive of gametocytemia with a ~14-day
528 delay[29]. Later, immunity prevents fast asexual growth and parasites that persist further are more
529 effectively removed in the spleen leading to sustained low parasitaemias. The ~5-12-day lag has
530 the opposite effect later in infection when asexual parasitaemia decreases and the proportion of
531 gametocytes reflects the parasitaemia of ~5-12 days earlier; all despite maintaining the same
532 sexual commitment rate.
533 In conclusion, our data is consistent with a model in which individuals not undergoing major lipid
534 deprivation, present a constant rate of *P. falciparum* sexual commitment as infections progress
535 from recently transmitted to persistent over several months.
536
537 **Methods**
538 **Gametocyte gene expression analysis.** We used RNAseq data of leucocyte-depleted blood
539 pellets from 12 children with asymptomatic malaria at the end of the dry season and an age- and
540 sex-matched cohort presenting with their first malaria case in the ensuing transmission season
541 reported in[11]. Originally 1456 gametocyte specific genes were reported[32], and we counted 1258
542 after excluding repetitions and converting nomenclature to its most recent version (Supplementary
543 Table 1). Out of these 1258 genes, we detected normalized reads of 551 gametocyte-specific
544 genes in the RNAseq data set[11] to perform a principal component analysis.
545
546 **Analysis of early and late gametocyte markers in RNA-seq data.** We compiled a list of early
547 and late gametocyte specific genes based on three RNA-seq studies comparing distinct parasite
548 stages, including data from Poran et al. 2017[33] obtained after request from the corresponding
549 author (compared day 2 versus day 9 of gametocytogenesis by single cell RNAseq); data from
550 Lopez-Barragan et al. 2011[34] (compared day 4 versus day 15 of gametocytogenesis by bulk
551 RNAseq) and data from Jeninga et al.[35] (compared day 4 of gametocytogenesis versus day 10 of
552 FACS sorted male and female gametocytes by bulk RNAseq). Poran et al. selected early and late
553 gametocyte genes as genes showing a 20-fold higher expression in early or late gametocytes over
554 the respective other group. Late gametocyte genes were also required to show a 20-fold higher
555 expression in late gametocytes compared to ring stage parasites, this was not the case for early
556 gametocyte genes. In Lopez-Barrgagan's data, early gametocyte genes were defined as genes
557 having a 10-fold expression increase in early gametocytes compared to late gametocytes. Genes

558 showing a 20-fold higher expression in late stages were designated as late gametocyte genes.
559 Expression differences to asexual stages were not considered. We revisited Jeninga et al. RNA-
560 Seq data for ring stage parasites, schizont stage parasites, day 4 and 10 male and female
561 gametocytes from GSE180985 and evaluated differential expression of sense transcripts. A
562 countmatrix was generated using Cufflinks (REF: doi:10.1038/nbt.1621). The matrix was analysed
563 by filtering for genes with at least 3-fold differential expression, and a cutoff of minimum 10 FPKM
564 per gene was applied. Intersecting the full list of all three publications describing early and late
565 gametocyte genes with genes transcribed in circulating parasites stages, defined by RNAseq data
566 of Andrade et al., generated a final list of 109 early and 172 late gametocyte genes to evaluate
567 expression differences of these genes between dry and rainy seasons. Intersecting the early and
568 late gametocyte list and all gametocyte genes reported by Painter et al., we obtained 551
569 gametocyte genes that were detected in the wet vs dry season RNAseq dataset[11]. Of these 343
570 were among differentially expressed determined using Deseq2 [62] (padj < 0.05, LFC >1). For GSEA,
571 differentially expressed genes between MAL and May were ranked by Log2 FC and analysed with
572 the fgsea [63] algorithm implemented in the clusterprofiler [64] R-package.
573
574 **Study subjects and ethical approval.** Approval by the Ethics Committee of Heidelberg University
575 Hospital, the Faculty of Medicine, Pharmacy and Odontostomatology (FMPOS) at the University of
576 Bamako, and the National Institute of Allergy and Infectious Diseases of the National Institutes of
577 Health Institutional Review Board was obtained to conduct the study registered at ClinicalTrials.gov
578 with the identifier NCT01322581. Clinical data and samples were obtained from 2012 to 2019 in a
579 cohort study previously described[65], conducted in Kalifabougou, Mali, where malaria transmission
580 occurs between June and December, and antimalarial drugs are provided by a single clinic and
581 pharmacy. All participants and the parents/guardians of included children provided written informed
582 consent. Exclusion criteria at enrolment included haemoglobin <7 g/dL, axillary temperature
583 ≥37.5°C, acute systemic illness, or use of antimalarial or immunosuppressive medications in the 30
584 days preceding enrolment. Clinical malaria cases were prospectively determined by passive
585 surveillance and defined by axillary temperature ≥37.5°C, ≥2500 asexual parasites/µL of blood,
586 and no other evident cause of fever. Malaria episodes were treated with a 3-day standard course of
587 artemether/lumefantrine according to Malian national guidelines. Cross-sectional clinical visits and
588 blood draws were performed late in the transmission season (October), and at the beginning
589 (January), mid (March) and end (May) of the dry season.
590
591 **Sample collection.** Venous blood (4 mL if donor age was below 4 years, and 8 mL if above) was
592 drawn by venepuncture on wet and dry season cross-sectional visits, and at first malaria episode of
593 the transmission season. Samples are referred as MAL for malaria cases or by time point of

594 collection. Blood was collected in sodium citrate-containing cell preparation tubes (Vacutainer CPT
595 Tubes, BD) and transported to the laboratory where RBC pellet and plasma were separated and
596 stored at −80°C within three hours of blood draw. Plasma used for lipidomic analysis and induction
597 of gametocytogenesis was separated by centrifugation and immediately frozen in liquid N_2.
598
599 **Parasite culture and preparation of a standard curve for gametocyte quantification.** Pf2004
600 parasites were cultured at 37° C in 5% O_2, 5% CO_2 and 90% N_2, at 5% haematocrit in RPMI-1640
601 medium (with L-glutamine and HEPES (Gibco)). Parasite culture medium was supplemented with
602 0.24% Sodium Bicarbonate (Gibco), 100µM Hypoxanthine (cc pro), 25 µg/mL gentamycin (Gibco)),
603 and 0.25% Albumax II (Gibco). Medium was changed daily, parasitaemia assessed by Giemsa-
604 stained blood smear and the culture split according to experimental needs.
605 *PfDyn*GFP/*PfP47*mCherry parasite lines[66] were cultured in presence of 15 µg/ml of Blasticidin-S-
606 HCL (Invitrogen) and 2 µM Pyrimethamine (Sigma Aldrich) as described for non-integrating
607 plasmids and P52 integrating plasmid. Parasites were grown to >4% parasitaemia when 50 mM N-
608 Acetylglucosamine (Sigma Aldrich) was added to the culture to eliminate asexual stages. After 4
609 consecutive days of N-Acetylglucosamine treatment, culture in complete RPMI was resumed.
610 Gametocyte development was monitored daily by smear, and on day 5 after start of gametocyte
611 induction magnetic enrichment was performed with MACS columns (Miltenyi Biotec). Gametocytes
612 were sorted on a BD FACSAria III on day 8, keeping cells at 4° C in suspended activation buffer,
613 (gating strategy in Supplementary Figure 2A). RNA of a defined numbers of sorted male and
614 female gametocytes was extracted and reverse transcribed, a standard curve prepared by serial
615 dilution and used for RT-qPCR as described below.
616
617 **RNA extraction and quantification of parasite transcripts.** RNA was isolated from 200 µl RBC
618 pellet by phenol-chloroform extraction using TRIzol (Ambion), followed by DNAse treatment using
619 the DNAse I Amplification Grade Enzyme (Invitrogen). RNA was quantified by absorption
620 measurements at 230, 260 and 280 nm on a Citation3 Imaging plate reader, or using the Qubit
621 RNA High Sensitivity kit (Thermo Scientific) followed by cDNA synthesis using the Superscript IV
622 Enzyme (Invitrogen) according to manufacturer instructions. A Taqman RT-qPCR multiplex assay
623 (Applied Biosystems) was performed on a qTower (Analytic Jena) with primers to quantify the
624 female gametocyte marker ookinete surface protein *pfs25* (PF3D7_1031000), the male gametocyte
625 transcript *pfmget* (Pf3D7_1469900), the master regulator of sexual commitment *ap2g*
626 (PF3D7_1222600) and a parasite housekeeping gene (*glycine-tRNA-ligase*, PF3D7_1420400).
627 We quantified primer efficiency and specificity with an NF54 parasite line expressing DyneinGFP
628 and carrying an episomal P47mCherry plasmid (DynGFP/P47mCherry) was used for sorting of
629 male and female gametocytes through their respective specific mCherry and/or GFP expression [38].

630 (Supplementary Figure 2a)
631 We generated standard curves of female or male gametocytes and asexual parasites by serial
632 dilution of cDNA of $1*10^6$ FACS-counted male and female gametocytes and asexual parasites in
633 10-fold dilution steps down to 10 parasites/gametocytes per ml. Using the standard curve,
634 amplification efficiency (E) was estimated using the equation $E = ((10^{\frac{-1}{slope}}) - 1) * 100$
635 (Supplementary Figure 2B). *pfs25* and *pfmget* expression was absent in asexual parasite and high
636 in sorted gametocytes was high and decreased with increasing dilution (Supplementary Figure 2b).
637 *pfmget* was approximately 10-fold higher expressed in male gametocytes (double+) compared to
638 females (mCherry+), consistent with 5-7% sorting impurity. (Supplementary Figure 2b) Log-linear
639 regression fit for the independent populations revealed a good fit with R^2-values of 0.94-0.98 for
640 *ap2-g*, 0.99 – 0.998 for *glycine-tRNA ligase*, 0.97-0.99 for *pfmget* and 0.997 -0.999 for *pfs25*.
641 Primer efficiencies for the 4 genes ranged from 97% (*pfs25*) to 115% *ap2g*) and were corrected for
642 in qPCR quantification. The combination of asexual and sexual standard curves was used for
643 qPCR quantification of total parasitaemias and female gametocytemia throughout the season. To
644 account for fluorescence leakage between channels a compensation matrix was calculated based
645 on single colour fluorescence measurements by an application specialist at Analytic Jena. *Gexp5*
646 (PF3D7_0936600) expression levels were quantified in a Taqman RT-qPCR duplex assay together
647 with *glycine-tRNA ligase* as a housekeeping gene. All primers and probes sequences are listed in
648 Supplementary Table 6. Relative quantification was performed by ΔΔCt method using *glycine-tRNA*
649 *ligase* as housekeeping gene and May samples a calibrator group. For all genes except *gexp5,*
650 primer Pfaffl correction was used in the quantification to account for different primer efficiencies [67].
651
652 **Phospholipid analysis.** May and MAL plasma samples (shown in Figure 1) were analysed by
653 shotgun lipidomics at Lipotype as described in[68]. Briefly, automated samples extraction was
654 followed by direct sample infusion and high-resolution Orbitrap mass spectrometry including lipid
655 class-specific internal standards to assure absolute quantification of LysoPC and LysoPE, using
656 LipotypeXplorer for identification of lipids in the mass spectra. Lipid species detected less than half
657 of samples were excluded, concentrations were normalized to total lipid amount in each sample.
658 Oct, Mar, May and MAL samples (shown in Figure 2 A,C) were analysed by Liquid
659 chromatography-mass spectrometry (LC-MS). Samples were extracted, processed, and analysed
660 at the Lipidomics Unit at the Institute of Physiological Chemistry in Mainz, using the liquid-liquid
661 extraction protocol as described[69]. All values were normalized to the analysed plasma volume.
662
663 **In vitro induction of *P. falciparum* sexual commitment and gametocytogenesis.** In vitro
664 induction of *P. falciparum* sexual commitment was performed as described by (Brancucci et al.,
665 2015). Pf2004 parasites were synchronized to a 4 h window by repeated treatment with 5% sorbitol

666 and MACS purification. Parasites at 26 ± 2 h post invasion (hpi) were plated on 48-well plates in
667 500 µl culture volume at 0.8-1% parasitaemia and 2.5% haematocrit and cultured in minimum fatty
668 acid medium (mFA, RPMI1640 with 100 µM hypoxanthine, 25 µg/ml gentamycin, 0.39% fatty-acid-
669 free BSA, 30 µM palmitic acid and 30 µM oleic acid) supplemented with 25% plasma from
670 asymptomatic children at the end of the dry season (PlMay), or 25% plasma from malaria cases
671 during the rainy season (PlMAL), in addition to the conditions used by Brancucci et al. (mFA alone,
672 and mFA supplemented with 25% German plasma (PlDE)). After 24 h of treatment, the medium
673 was changed to culture medium and subsequently changed daily. At 48 h after beginning of
674 treatment 30 IU/ml heparin were added to block re-invasion of parasites and eliminate asexual
675 forms. At 0, 48 and 120 h post treatment RBC pellets were collected for parasitaemia and
676 gametocytaemia determination by flow cytometry (50 µl of culture stained with 5x SYBR Green II
677 (Invitrogen) and 7,5 µM MitoTracker (Applied Biosystems) for 30 min at 37 °C and acquired with
678 CountBright Absolute Counting Beads (Thermo Ficher) on a FACS Canto II or an LSR II and
679 analysed using FlowJo software 10.2 or higher versions (Tree Star)). Additionally, Giemsa-stained
680 blood smears were prepared at 48 h and 120 h post-treatment and blindly analysed by microscopy,
681 counting RBCs, parasites, and gametocytes in 18 fields of view. Multiplication rate of parasites was
682 calculated as $\frac{parasitemia\ 48\ h}{parasitemia\ 0\ h}$, and conversion rate as $\frac{gametocytemia\ 120\ h}{parasitemia\ 48\ h}$.
683
684 **Quantification of parasites in samples of Ugandan asymptomatic carriers by RT-qPCR.** We
685 compared the Malian data from dry and wet season with data from 150 Ugandan individuals
686 enrolled in a 2-year longitudinal study including monthly standardized clinical evaluation and blood
687 collection[37] retrieved from ClinEpiDB
688 (https://clinepidb.org/ce/app/record/dataset/DS_51b40fe2e2122). Asymptomatic *P. falciparum*
689 positive individuals (20.4 years ± 17.2, median: 13.3 years) were included based on the following
690 criteria: i) ≥ two PCR+ time points, ii) ≤ 3 negative time points in between positive, iii) same clone
691 (determined by deep amplicon sequencing of atypical membrane antigen 1 (*ama1*) as described
692 in[70] present at all time points of one asymptomatic infection. Additionally, we used samples from an
693 age-matched group of 38 clinical malaria cases (tympanic temperature > 38°C or history of fever in
694 the previous 24 hours and *P. falciparum* positivity by microscopy). *P. falciparum* parasite and
695 gametocyte density in blood samples were measured by qPCR of multi copy conserved *var* gene
696 acidic terminal sequence[71] and *ccp4* (PF3D7_0903800), respectively. Average levels of
697 parasitaemia and gametocytaemia during each asymptomatic infection, were estimated as the area
698 under curve over the course of infection divided by length of infection. For symptomatic infections,
699 only the quantification before treatment on day of diagnosis was considered.
700

701 **Mathematical model.** The developed mathematical model extends a model used previously to
702 describe asexual parasite and gametocytes dynamics [31]. The model considers 3 different main
703 parasite populations, i.e., distinguishing between asexual parasites (P), sexually committed
704 parasites (P_G) and gametocytes (G) (Fig 4E). Asexual parasites develop and replicate within a
705 red blood cell over a cycle of length a_L=48h after which mature schizonts burst and release a
706 number of r_P=18-32 merozoites that are able to invade new red blood cells. During this
707 replication cycle, parasites are assumed to be removed through splenic clearance and active
708 immune response. In extension to the previous model, we assume that this removal of asexual
709 and committed parasites follows an age dependent death rate, σ_a that differs in distinct phases
710 of acute and chronic *P. falciparum* infection. The following iterative equation describes asexual
711 parasite growth at discrete time steps for parasite age, *a*, and time, *t*, increments of one hour.

712
$$P(a,t) = \begin{cases} P(a-1,t-1)e^{-\sigma_a} \ , a = 2,3,\dots,a_L \\ r_p \ P(a_L,t-1)e^{-\sigma_a} \ , a = 1 \end{cases} \quad (1)$$

713
$$P(a_s + 1,t) = (1-f)P(a_s,t-1)e^{-\sigma_a} \quad (2)$$

714

715 The rate of parasite removal, σ_a, is assumed to increase with parasite age within one replicative
716 cycle and is described by a sigmoidal curve given by:

717
$$\sigma_a = \sigma(a) = \frac{\sigma_{max}}{1+e^{p_\sigma(T_\sigma - a)}} \quad (3)$$

718 The parameter σ_{max} defines the maximal rate of parasite removal, T_σ, the age at which 50% of
719 parasites are removed, and p_σ a scaling parameter.

720 At parasite trophozoite stage of a_s= 20hpi parasites adhere to the endothelium when at the
721 same time a fraction, f, of parasites enters sexual commitment. Committed parasites continue
722 the rest of the replication cycle producing only committed parasites that enter the first
723 gametocyte stage at the sequestration age, a_s, of the following replication cycle
724

725
$$P_G(a_s+1,t) = f\ P(a_s,t-1)e^{-\sigma_a} \quad (4)$$

726
$$P_G\ (a,t) = \begin{cases} P(a-1,t-1)e^{-\sigma_a}, a = 2,3,\dots,a_L \ except\ a = a_s\ and\ a = \ a_s+1 \\ r_p \ P(a_L,t-1)e^{-\sigma_a} \ , a = 1 \end{cases} \quad (5)$$

727

728 Gametocyte development through five stages, of which only stage 5 is found in circulation, is
729 modelled by:
730

$$G_1(t) = G_1(t-1)e^{-(m-\delta_G)} + \frac{P_G(a_s-1,t-1)e^{-\sigma_a}(1-e^{-(m+\delta_G)})}{m+\delta_G} \quad (6)$$

731

$$G_2(t) = G_2(t-1)e^{-(m-\delta_G)} + \frac{mG_1\ (t-1)\ (1-e^{-(m+\delta_G)})}{m+\delta_G} \quad (7)$$

732

$$G_3(t) = G_3(t-1)e^{-(m-\delta_G)} + \frac{mG_2\ (t-1)\ (1-e^{-(m+\delta_G)})}{m+\delta_G} \quad (8)$$

733
734

$$G_4(t) = G_4(t-1)e^{-(m-\delta_G)} + \frac{mG_3\ (t-1)\ (1-e^{-(m+\delta_G)})}{m+\delta_G} \quad (9)$$

735

$$G_5(t) = G_5(t-1)e^{-(\delta_{G5})} + \frac{mG_4\ (t-1)\ (1-e^{-(\delta_{G5})})}{\delta_{G5}} \quad (10)$$

736
737 Immature gametocytes, that are sequestered, mature with a maturation rate, m, and are lost
738 by death rate δ_G , while mature circulating gametocytes are removed by a splenic clearance
739 rate δ_{G5}. As pointed out above the whole model is simulated by discrete time-steps of one-
740 hour increments.
741 Our model assumes two stages of *P. falciparum* infection, accounting for an acute and a chronic
742 asymptomatic phase. The start of the infection is marked by the beginning of blood stage infection,
743 for which we assume an initial parasite load, IPL, with parasite age normally distributed with mean,
744 μ_{IPL} and standard deviation σ_{IPL}. During the acute phase of infection parasitaemias increase rapidly
745 leading to clinical symptoms within the first 2 weeks of blood stage infection[72]. At 14 days after the
746 start of blood stage infection, the maximal parasite removal rate is assumed to increase to σ_{max2} to
747 account for the onset of an effective adaptive immune response and, thus, an increase in age-
748 dependent parasite loss. This timepoint indicates the beginning of the chronic phase of infection.
749

The model described in Eqs (1-10) was applied to the data on symptomatic and asymptomatic log-transformed parasitaemias and gametocytemias of the Malian cohort assuming a fixed parasite life-cycle period of a_L=48h, a replication factor of 25, a sequestration age of a_S= 20hpi, as well as T_σ=32h and P_σ=0.7 characterizing age-dependent parasite removal during the acute infection phase. For the initial parasite load, IPL, we assume a fixed Gaussian parasite age distribution with parasite mean age m_{IPL}=7h and standard deviation σ_{IPL}=5.5. All remaining parameters were fitted to both symptomatic and asymptomatic time points simultaneously using an approximative Bayesian computing approach (pyABC, Klinger et al. Bioinformatics 2018 [73]). Prior distributions for the individual parameters spanning biologically realistic ranges (Supplementary Table 2), as well as all fixed parameters (Supplementary Table 3) were selected in accordance with previous studies. pyABC was run with the following stopping parameters: ε_{min}=0.01, maximal population size pop_{max}=100, $\Delta\varepsilon_{min}$= 0.05. Given the complexity of the model and the available data, parameter posterior distributions are reported for the 10th pyABC-generation of several independent pyABC fitting runs in order to check robustness of results and avoid local convergence of algorithms (Supplementary Figure 3). Using the $\Delta\varepsilon_{min}$-criterion for stopping did not change the overall conclusions.

To test model sensitivity with regard to the fixed parameter values, we examined the effect of using the high and low boundaries for the reported estimates for each of the constants on posterior parameter distributions. While expected dependencies of the replication rate, r_P , and σ_{T} with the removal rates σ_{max} and σ_{max2}, could be observed, the overall posterior parameter distributions for the free parameters proved stable to changes in model constants (Supplementary Fig. 4).

The parasite multiplication factor was calculated by $r_p e^{-total\ clearance}(1-f)$ with the term $e^{-total\ clearance}$ describing cumulative clearance per replication cycle. Gametocyte sequestration time was calculated by $\frac{4}{m}$ in relation to the 4 sequestered states (stage I to IV) [74].

For scenario 2 and scenario 3, the model framework was modified by assuming a change in the fraction of parasites entering sexual commitment, f, at different timepoints. In scenario 2, f was assumed to change to f_2 at day 100 after infection, while in scenario 3, we assumed a deviating fraction f_3 from day 7 to day 21. All other parameter and model constants were left unchanged, and parameter fits were performed with the same pyABC-settings as before, assuming the same prior distributions for f_2 and f_3 as for the parameter f.

For model comparison, the Bayesian Information Criterion (BIC) was calculated by $BIC = -2\mathrm{LL} + klog(n)$ with *k* being the number of free parameters and *n* the number of data points. The log likelihood was calculated as the sum of each gametocytemia and parasitemia measurement

calculated using a normal distribution as $\ell(\theta) = -\frac{1}{2}n\log(2\pi\sigma^2) - \sum_{i=1}^{n}\frac{(y_i - f(x_i,\theta))^2}{2\sigma^2}$ where σ^2 is the variance, y_i the corresponding measurement at time point , x_i and $f(x_i,\theta)$ the model output. The BIC in scenario 1 with an unchanged commitment rate was slightly lower than in the other two scenarios, due to the lower number of free parameters (Supplementary Fig. 5A). In general, several of the model parameters cannot be independently determined showing correlations between several of the parameter estimates including between the initial parasite load IPL and the removal rates $\sigma_{\max}$ and $\sigma_{\max 2}$, respectively, as well as between the two removal rates $\sigma_{\max}$ and $\sigma_{\max 2}$ (Supplementary Fig. 5B). These correlations are expected from the model structure inhibiting their independent inference. Of note, we did not observe a strong correlation between the fraction of committing parasites f, f_2, and f_3 and any of the other parameters (Supplementary Fig. 5B). We assessed robustness of the parameter estimates obtained by pyABC by running the fitting algorithm 100 times for each of the three scenarios and compared parameter estimates in the 10th generation. For all three scenarios, parameter estimates in the 100 fitting runs followed a smooth distribution not indicating the convergence of the runs towards different local minima (Supplementary Fig. 6 A and B) [11,31]. All code to run and analyse the mathematical model is available at https://github.com/GrawLab/MalariaReplication.

Supplementary Table 1: Gametocyte-related genes published in Painter et al. [32], Poran et al. 2017[33], Lopez-Barragan et al. 2011[34] and Jeninga et al.[35] and their expression in end-dry season asymptomatic infections and clinical malaria cases published in Andrade et al. 2020 [11]. Data is available upon request.

Supplementary Table 2: Parameter prior ranges

Parameter	Unit	Description	Prior range	Reference
$\boldsymbol{IPL}$	Parasites/ml	Initial parasite load	100 - 1000	(Mouwenda et al 2024)[75]
$\boldsymbol{\sigma_{\max}}$	h^{-1}	Maximal removal rates during acute phase	0.01-0.15	(Andrade et al 2020) [11]
$\boldsymbol{\sigma}_{\max 2}$	h^{-1}	Maximal removal rates during chronic phase	0.01-0.4	
$\boldsymbol{\delta_G}$	h^{-1} (*10^{-4})	Death rate immature gametocytes	0.1 – 1	(Cao et al. 2019) [74]
$\boldsymbol{\delta_{G5}}$	h^{-1} (*10^{-2})	Death rate mature gametocytes	0.135 – 3.25	(Cao et al 2019, Eichner et al 2001) [42,74]
$\boldsymbol{m}$	h^{-1} (*10^{-2})	Gametocyte maturation rate	1.38 - 4.1	(Cao et al 2019, Eichner et al 2001) [42,74]
$\boldsymbol{f}$	h^{-1} (*10^{-2})	Commitment rate	0.1 - 1.0	(Cao et al 2019, Eichner et al 2001) [42,74]
$\boldsymbol{f_2}$, $\boldsymbol{f_3}$	h^{-1} (*10^{-2})$h - 1\ (*10 - 2)$	Modified commitment rate$Modified\ commitment\ rate$	0.1 - 1.0 0.1 – 1.0	(Cao et al 2019, Eichner et al 2001) [42,74]

Supplementary Table 3: Model constants

Constant	Unit	Description	Prior range	Reference for prior range
μ_{IPL}	h	Initial parasite age	7	(Eichner et al 2001) [42]
σ_{IPL}	h	Standard deviation of initial parasite age	5.5	(Cao et al 2019) [74]
r_p		Replication factor	25	
a_L	h	Life cycle length	48	
a_S	h	Sequestration age	20	
T_S	h	Age at which 50% of parasites are removed	32	(Andrade et al 2020) [11]
P_s		Shape parameter	0.7	(Andrade et al 2020) [11]

Supplementary Table 4: 89% CI of posterior parameter distribution

Parameter	Unit	Scenario 1	Scenario 2	Scenario 3
IPL	Parasites/ml	264 - 1020	311 - 1060	276 - 1010
σ_{max}	h^{-1}	0.128 - 0.142	0.126 - 0.142	0.128 - 0.141
σ_{max2}	h^{-1} (*10^{-2})	5.46 - 6.91	5.49 - 723	5.52 - 6.89
δ_G	h^{-1} (*10^{-4})	0.273- 0.987	0.215 - 0.91	0.285 - 0.974
δ_{G5}	h^{-1} (*10^{-2})	1.74 – 3.34	2.15 – 3.32	1.85 – 3.37
m	h^{-1} (*10^{-2})	3.47 – 5.46	3.08 – 5.45	2.1 – 5.21
f	h^{-1} (*10^{-2})	0.11 – 0.404	0.104 – 0.376	0.193 – 0.896
f_2, f_3	h^{-1} (*10^{-2})		0.348 – 1.01	0.109 – 0.324

Acknowledgments

We thank the residents of Kalifabougou, Mali and Nangonera, Uganda for participating in the studies. We acknowledge the support of the Flow Cytometry Core Facility of DKFZ, the Heidelberg University Metabolomics Core Technology Platform, and the Clinical Lipidomics Unit of Mainz University Medical Center. We thank Matthias Marti and Lauriane Sollelis at University of Glasgow for help and expertise with in vitro induction of parasite sexual commitment and gametocytogenesis. This work was supported by the European Research Council (ERC) under the European Union's Horizon 2020 research and innovation programme (grant agreement No 759534), and the German Center for Infection research (DZIF). The Malian cohort study was supported by the Division of Intramural Research, National Institute of Allergy and Infectious Diseases of the National Institutes of Health; and the Ugandan study was supported by the National Institutes of Health as part of the International Centers of Excellence in Malaria Research program. Chica and Heinz-Schaller Foundation supported Frederik Graw.

Data Availability

The RNA-seq data analyzed during the current study are available through (1) NCBI's Gene Expression Omnibus (https://www.ncbi.nlm.nih.gov/geo/) under GEO Series accession number GSE148125 (Andrade et al. 2020), GSE72695 (Painter et al. 2018), GSE180985 (Jeninga et al. 2023); (2) GanBank with accession number SRP009370 (Lopez-Barrangan et al. 2011); and (3) NCBI Sequence Read Archive under accession code SRP116718 (Poran et al.).

Competing Interest Statement

The authors declare that they have no conflict of interest.

References

1 Grassi, B., Bignami, A. & Bastianelli, G. Medical Zoology: Further Researches upon the Cycle of Human Malaria in the Body of the Mosquito. *Ind Med Gaz* **34**, 104-107 (1899).

2 Kafsack, B. F. *et al.* A transcriptional switch underlies commitment to sexual development in malaria parasites. *Nature* **507**, 248-252 (2014). https://doi.org:10.1038/nature12920

3 Bruce, M. C., Alano, P., Duthie, S. & Carter, R. Commitment of the malaria parasite Plasmodium falciparum to sexual and asexual development. *Parasitology* **100 Pt 2**, 191-200 (1990). https://doi.org:10.1017/s0031182000061199

4 Inselburg, J. Gametocyte formation by the progeny of single Plasmodium falciparum schizonts. *J Parasitol* **69**, 584-591 (1983).

5 Hawking, F., Wilson, M. E. & Gammage, K. Evidence for cyclic development and short-lived maturity in the gametocytes of Plasmodium falciparum. *Trans R Soc Trop Med Hyg* **65**, 549-559 (1971). https://doi.org:10.1016/0035-9203(71)90036-8

6 Farfour, E., Charlotte, F., Settegrana, C., Miyara, M. & Buffet, P. The extravascular compartment of the bone marrow: a niche for Plasmodium falciparum gametocyte maturation? *Malar J* **11**, 285 (2012). https://doi.org:10.1186/1475-2875-11-285

7 Tiburcio, M. *et al.* Early gametocytes of the malaria parasite Plasmodium falciparum specifically remodel the adhesive properties of infected erythrocyte surface. *Cell Microbiol* **15**, 647-659 (2013). https://doi.org:10.1111/cmi.12062

8 Smalley, M. E. & Sinden, R. E. Plasmodium falciparum gametocytes: their longevity and infectivity. *Parasitology* **74**, 1-8 (1977). https://doi.org:10.1017/s0031182000047478

9 Gebru, T., Lalremruata, A., Kremsner, P. G., Mordmuller, B. & Held, J. Life-span of in vitro differentiated Plasmodium falciparum gametocytes. *Malar J* **16**, 330 (2017). https://doi.org:10.1186/s12936-017-1986-6

10 Dicko, A. *et al.* The etiology of severe anemia in a village and a periurban area in Mali. *Blood* **104**, 1198-1200 (2004).

11 Andrade, C. M. *et al.* Increased circulation time of Plasmodium falciparum underlies persistent asymptomatic infection in the dry season. *Nat Med* (2020). https://doi.org:10.1038/s41591-020-1084-0

12 Babiker, H. A., Abdel-Muhsin, A. M., Ranford-Cartwright, L. C., Satti, G. & Walliker, D. Characteristics of Plasmodium falciparum parasites that survive the lengthy dry season in eastern Sudan where malaria transmission is markedly seasonal. *Am J Trop Med Hyg* **59**, 582-590 (1998). https://doi.org:10.4269/ajtmh.1998.59.582

13 Portugal, S. *et al.* Treatment of Chronic Asymptomatic Plasmodium falciparum Infection Does Not Increase the Risk of Clinical Malaria Upon Reinfection. *Clin Infect Dis* **64**, 645-653 (2017). https://doi.org:10.1093/cid/ciw849

14 Adomako-Ankomah, Y. *et al.* Host age and Plasmodium falciparum multiclonality are associated with gametocyte prevalence: a 1-year prospective cohort study. *Malar J* **16**, 473 (2017). https://doi.org:10.1186/s12936-017-2123-2

15 Drakeley, C. J., Secka, I., Correa, S., Greenwood, B. M. & Targett, G. A. Host haematological factors influencing the transmission of Plasmodium falciparum gametocytes to Anopheles

gambiae s.s. mosquitoes. *Trop Med Int Health* **4**, 131-138 (1999). https://doi.org:10.1046/j.1365-3156.1999.00361.x

16 Gouagna, L. C. *et al.* Genetic variation in human HBB is associated with Plasmodium falciparum transmission. *Nat Genet* **42**, 328-331 (2010). https://doi.org:10.1038/ng.554

17 Price, R. *et al.* Risk factors for gametocyte carriage in uncomplicated falciparum malaria. *Am J Trop Med Hyg* **60**, 1019-1023 (1999). https://doi.org:10.4269/ajtmh.1999.60.1019

18 Barry, A. *et al.* Higher gametocyte production and mosquito infectivity in chronic compared to incident Plasmodium falciparum infections. *Nat Commun* **12**, 2443 (2021). https://doi.org:10.1038/s41467-021-22573-7

19 Group, W. G. S. Gametocyte carriage in uncomplicated Plasmodium falciparum malaria following treatment with artemisinin combination therapy: a systematic review and meta-analysis of individual patient data. *BMC Med* **14**, 79 (2016). https://doi.org:10.1186/s12916-016-0621-7

20 Rek, J. *et al.* Asymptomatic school-aged children are important drivers of malaria transmission in a high endemicity setting in Uganda. *J Infect Dis* (2022). https://doi.org:10.1093/infdis/jiac169

21 Tadesse, F. G. *et al.* The Relative Contribution of Symptomatic and Asymptomatic Plasmodium vivax and Plasmodium falciparum Infections to the Infectious Reservoir in a Low-Endemic Setting in Ethiopia. *Clin Infect Dis* **66**, 1883-1891 (2018). https://doi.org:10.1093/cid/cix1123

22 Andolina, C. *et al.* Plasmodium falciparum gametocyte carriage in longitudinally monitored incident infections is associated with duration of infection and human host factors. *Sci Rep* **13**, 7072 (2023). https://doi.org:10.1038/s41598-023-33657-3

23 Williams, J. L. Stimulation of Plasmodium falciparum gametocytogenesis by conditioned medium from parasite cultures. *Am J Trop Med Hyg* **60**, 7-13 (1999). https://doi.org:10.4269/ajtmh.1999.60.7

24 Dyer, M. & Day, K. P. Regulation of the rate of asexual growth and commitment to sexual development by diffusible factors from in vitro cultures of Plasmodium falciparum. *Am J Trop Med Hyg* **68**, 403-409 (2003).

25 Brancucci, N. M. B. *et al.* Lysophosphatidylcholine Regulates Sexual Stage Differentiation in the Human Malaria Parasite Plasmodium falciparum. *Cell* **171**, 1532-1544 e1515 (2017). https://doi.org:10.1016/j.cell.2017.10.020

26 Filarsky, M. *et al.* GDV1 induces sexual commitment of malaria parasites by antagonizing HP1-dependent gene silencing. *Science* **359**, 1259-1263 (2018). https://doi.org:10.1126/science.aan6042

27 Campelo Morillo, R. A. *et al.* The transcriptional regulator HDP1 controls expansion of the inner membrane complex during early sexual differentiation of malaria parasites. *Nat Microbiol* **7**, 289-299 (2022). https://doi.org:10.1038/s41564-021-01045-0

28 Harris, C. T. *et al.* Sexual differentiation in human malaria parasites is regulated by competition between phospholipid metabolism and histone methylation. *Nature Microbiology* (2023). https://doi.org:10.1038/s41564-023-01396-w

29 Blanken, S. L. *et al.* Plasmodium falciparum gametocyte production correlates with genetic markers of parasite replication but is not influenced by experimental exposure to mosquito biting. *EBioMedicine* **105**, 105190 (2024). https://doi.org:10.1016/j.ebiom.2024.105190

30 Thomson-Luque, R. *et al.* Plasmodium falciparum transcription in different clinical presentations of malaria associates with circulation time of infected erythrocytes. *Nat Commun* **12**, 4711 (2021). https://doi.org:10.1038/s41467-021-25062-z

31 Cao, P. *et al.* Modeling the dynamics of Plasmodium falciparum gametocytes in humans during malaria infection. *Elife* **8** (2019). https://doi.org:10.7554/eLife.49058

32 Painter, H. J., Carrasquilla, M. & Llinas, M. Capturing in vivo RNA transcriptional dynamics from the malaria parasite Plasmodium falciparum. *Genome Res* **27**, 1074-1086 (2017). https://doi.org:10.1101/gr.217356.116

33 Poran, A. *et al.* Single-cell RNA sequencing reveals a signature of sexual commitment in malaria parasites. *Nature* **551**, 95-99 (2017). https://doi.org:10.1038/nature24280

34 Lopez-Barragan, M. J. *et al.* Directional gene expression and antisense transcripts in sexual and asexual stages of Plasmodium falciparum. *BMC Genomics* **12**, 587 (2011). https://doi.org:10.1186/1471-2164-12-587

35 Jeninga, M. D. *et al.* Plasmodium falciparum gametocytes display global chromatin remodelling during sexual differentiation. *BMC Biol* **21**, 65 (2023). https://doi.org:10.1186/s12915-023-01568-4

36 Andrade, C. M. *et al.* Infection length and host environment influence on Plasmodium falciparum dry season reservoir. *EMBO Mol Med* (2024). https://doi.org:10.1038/s44321-024-00127-w

37 Andolina, C. *et al.* Sources of persistent malaria transmission in a setting with effective malaria control in eastern Uganda: a longitudinal, observational cohort study. *Lancet Infect Dis* (2021). https://doi.org:10.1016/S1473-3099(21)00072-4

38 Meerstein-Kessel, L. *et al.* A multiplex assay for the sensitive detection and quantification of male and female Plasmodium falciparum gametocytes. *Malar J* **17**, 441 (2018). https://doi.org:10.1186/s12936-018-2584-y

39 Ruhamyankaka, E. *et al.* ClinEpiDB: an open-access clinical epidemiology database resource encouraging online exploration of complex studies. *Gates Open Res* **3**, 1661 (2019). https://doi.org:10.12688/gatesopenres.13087.2

40 Mueller, I. *et al.* Force of infection is key to understanding the epidemiology of Plasmodium falciparum malaria in Papua New Guinean children. *Proceedings of the National Academy of Sciences* **109**, 10030-10030 (2012). https://doi.org:10.1073/pnas.1200841109

41 Hofmann, N. E. *et al.* The complex relationship of exposure to new Plasmodium infections and incidence of clinical malaria in Papua New Guinea. *eLife* **6** (2017). https://doi.org:10.7554/ELIFE.23708

42 Eichner, M. *et al.* Genesis, sequestration and survival of Plasmodium falciparum gametocytes: parameter estimates from fitting a model to malariatherapy data. *Trans R Soc Trop Med Hyg* **95**, 497-501 (2001). https://doi.org:10.1016/s0035-9203(01)90016-1

43 Childs, L. M. & Buckee, C. O. Dissecting the determinants of malaria chronicity: why within-host models struggle to reproduce infection dynamics. *J R Soc Interface* **12**, 20141379-20141379 (2015). https://doi.org:10.1098/rsif.2014.1379

44 Tiburcio, M. *et al.* Specific expression and export of the Plasmodium falciparum Gametocyte EXported Protein-5 marks the gametocyte ring stage. *Malar J* **14**, 334 (2015). https://doi.org:10.1186/s12936-015-0853-6

45 Usui, M. *et al.* Plasmodium falciparum sexual differentiation in malaria patients is associated with host factors and GDV1-dependent genes (vol 10, 2140, 2019). *Nature Communications* **10** (2019). https://doi.org:ARTN 2740

10.1038/s41467-019-10805-w

46 Shanks, G. D. Hypothesis: dynamics of classical malaria epidemics show Plasmodium falciparum's survival strategy. *Am J Trop Med Hyg* **92**, 561-564 (2015). https://doi.org:10.4269/ajtmh.14-0541

47 Rono, M. K. *et al.* Adaptation of Plasmodium falciparum to its transmission environment. *Nat Ecol Evol* **2**, 377-387 (2018). https://doi.org:10.1038/s41559-017-0419-9

48 Abdi, A. I. *et al.* Plasmodium falciparum adapts its investment into replication versus transmission according to the host environment. *Elife* **12** (2023). https://doi.org:10.7554/eLife.85140

49 Oduma, C. O. *et al.* Increased investment in gametocytes in asymptomatic Plasmodium falciparum infections in the wet season. *BMC Infect Dis* **21**, 44 (2021). https://doi.org:10.1186/s12879-020-05761-6

50 Rosenberg, R., Andre, R. G. & Ketrangsee, S. Seasonal fluctuation of Plasmodium falciparum gametocytaemia. *Trans R Soc Trop Med Hyg* **84**, 29-33 (1990). https://doi.org:10.1016/0035-9203(90)90369-p

51 Gadalla, A. A. H. *et al.* Associations between Season and Gametocyte Dynamics in Chronic Plasmodium falciparum Infections. *Plos One* **11** (2016). https://doi.org:ARTN e0166699

10.1371/journal.pone.0166699

52 Ouedraogo, A. L. *et al.* Seasonal patterns of Plasmodium falciparum gametocyte prevalence and density in a rural population of Burkina Faso. *Acta Trop* **105**, 28-34 (2008). https://doi.org:10.1016/j.actatropica.2007.09.003

53 Ouedraogo, A. L. *et al.* Dynamics of the Human Infectious Reservoir for Malaria Determined by Mosquito Feeding Assays and Ultrasensitive Malaria Diagnosis in Burkina Faso. *J Infect Dis* **213**, 90-99 (2016). https://doi.org:10.1093/infdis/jiv370

54 Portugaliza, H. P. *et al.* Artemisinin exposure at the ring or trophozoite stage impacts Plasmodium falciparum sexual conversion differently. *Elife* **9** (2020). https://doi.org:10.7554/eLife.60058

55 Orikiiriza, J. *et al.* Lipid response patterns in acute phase paediatric Plasmodium falciparum malaria. *Metabolomics* **13**, 41 (2017). https://doi.org:10.1007/s11306-017-1174-2

56 Cruz Camacho, A. *et al.* High-throughput analysis of the transcriptional patterns of sexual genes in malaria. *Parasit Vectors* **16**, 14 (2023). https://doi.org:10.1186/s13071-022-05624-w

57 Stewart, L. B. *et al.* Plasmodium falciparum Sexual Commitment Rate Variation among Clinical Isolates and Diverse Laboratory-Adapted Lines. *Microbiology Spectrum* **10** (2022). https://doi.org:10.1128/spectrum.02234-22

58 Portugaliza, H. P. *et al.* Plasmodium falciparum sexual conversion rates can be affected by artemisinin-based treatment in naturally infected malaria patients. *EBioMedicine* **83**, 104198 (2022). https://doi.org:10.1016/j.ebiom.2022.104198

59 Greischar, M. A., Mideo, N., Read, A. F. & Bjornstad, O. N. Quantifying Transmission Investment in Malaria Parasites. *PLoS Comput Biol* **12**, e1004718 (2016). https://doi.org:10.1371/journal.pcbi.1004718

60 Prajapati, S. K. *et al.* The transcriptome of circulating sexually committed Plasmodium falciparum ring stage parasites forecasts malaria transmission potential. *Nat Commun* **11**, 6159 (2020). https://doi.org:10.1038/s41467-020-19988-z

61 Collins, W. E. & Jeffery, G. M. A retrospective examination of sporozoite- and trophozoite-induced infections with Plasmodium falciparum: development of parasitologic and clinical immunity during primary infection. *Am J Trop Med Hyg* **61**, 4-19 (1999). https://doi.org:10.4269/tropmed.1999.61-04

62 Love, M. I., Huber, W. & Anders, S. Moderated estimation of fold change and dispersion for RNA-seq data with DESeq2. *Genome Biology* **15**, 550-550 (2014). https://doi.org:10.1186/s13059-014-0550-8

63 Korotkevich, G. *et al.* Fast gene set enrichment analysis. *bioRxiv*, 060012 (2021). https://doi.org:10.1101/060012

64 Yu, G., Wang, L.-G., Han, Y. & He, Q.-Y. clusterProfiler: an R Package for Comparing Biological Themes Among Gene Clusters. *OMICS: A Journal of Integrative Biology* **16**, 284-287 (2012). https://doi.org:10.1089/omi.2011.0118

65 Tran, T. M. *et al.* An intensive longitudinal cohort study of Malian children and adults reveals no evidence of acquired immunity to Plasmodium falciparum infection. *Clin Infect Dis* **57**, 40-47 (2013). https://doi.org:10.1093/cid/cit174

66 Lasonder, E. *et al.* Integrated transcriptomic and proteomic analyses of P. falciparum gametocytes: molecular insight into sex-specific processes and translational repression. *Nucleic Acids Res* **44**, 6087-6101 (2016). https://doi.org:10.1093/nar/gkw536

67 Pfaffl, M. W. A new mathematical model for relative quantification in real-time RT-PCR. *Nucleic Acids Res* **29**, e45 (2001). https://doi.org:10.1093/nar/29.9.e45

68 Surma, M. A. *et al.* An automated shotgun lipidomics platform for high throughput, comprehensive, and quantitative analysis of blood plasma intact lipids. *Eur J Lipid Sci Technol* **117**, 1540-1549 (2015). https://doi.org:10.1002/ejlt.201500145

69 Lerner, R., Post, J., Loch, S., Lutz, B. & Bindila, L. Targeting brain and peripheral plasticity of the lipidome in acute kainic acid-induced epileptic seizures in mice via quantitative mass spectrometry. *Biochim Biophys Acta Mol Cell Biol Lipids* **1862**, 255-267 (2017). https://doi.org:10.1016/j.bbalip.2016.11.008

70 Briggs, J. *et al.* Sex-based differences in clearance of chronic Plasmodium falciparum infection. *Elife* **9** (2020). https://doi.org:10.7554/eLife.59872

71 Hofmann, N. *et al.* Ultra-sensitive detection of Plasmodium falciparum by amplification of multi-copy subtelomeric targets. *PLoS Med* **12**, e1001788 (2015). https://doi.org:10.1371/journal.pmed.1001788

72 Tran, T. M. *et al.* A Molecular Signature in Blood Reveals a Role for p53 in Regulating Malaria-Induced Inflammation. *Immunity* **51**, 750-765 e710 (2019). https://doi.org:10.1016/j.immuni.2019.08.009

1050 73 Klinger, E., Rickert, D. & Hasenauer, J. pyABC: distributed, likelihood-free inference.
1051 *Bioinformatics* **34**, 3591-3593 (2018). https://doi.org:10.1093/bioinformatics/bty361
1052 74 Cao, P. *et al.* Modeling the dynamics of Plasmodium falciparum gametocytes in humans during
1053 malaria infection. *Elife* **8**, e49058-e49058 (2019). https://doi.org:10.7554/eLife.49058
1054 75 Mouwenda, Y. D. *et al.* Immune responses associated with protection induced by
1055 chemoattenuated PfSPZ vaccine in malaria-naive Europeans. *JCI Insight* **9** (2024).
1056 https://doi.org:10.1172/jci.insight.170210

1057

1058

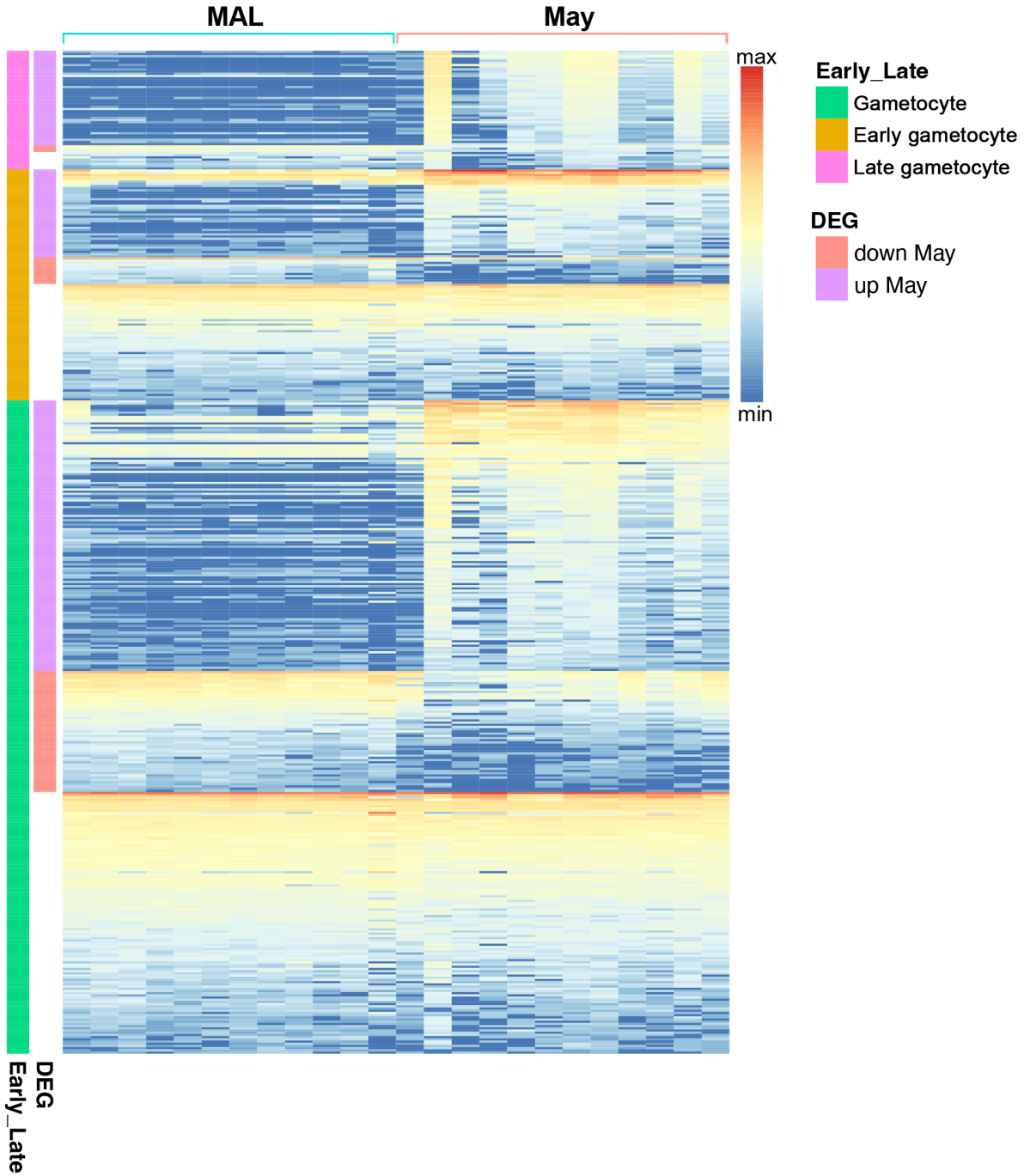

Supplementary Figure 1
Heatmap showing normalized reads of 551 gametocyte specific genes of *P. falciparum* (rows) for each subject (columns) collected at the end of the dry season (May) and at the first clinical malaria case (MAL) in the ensuing transmission season.

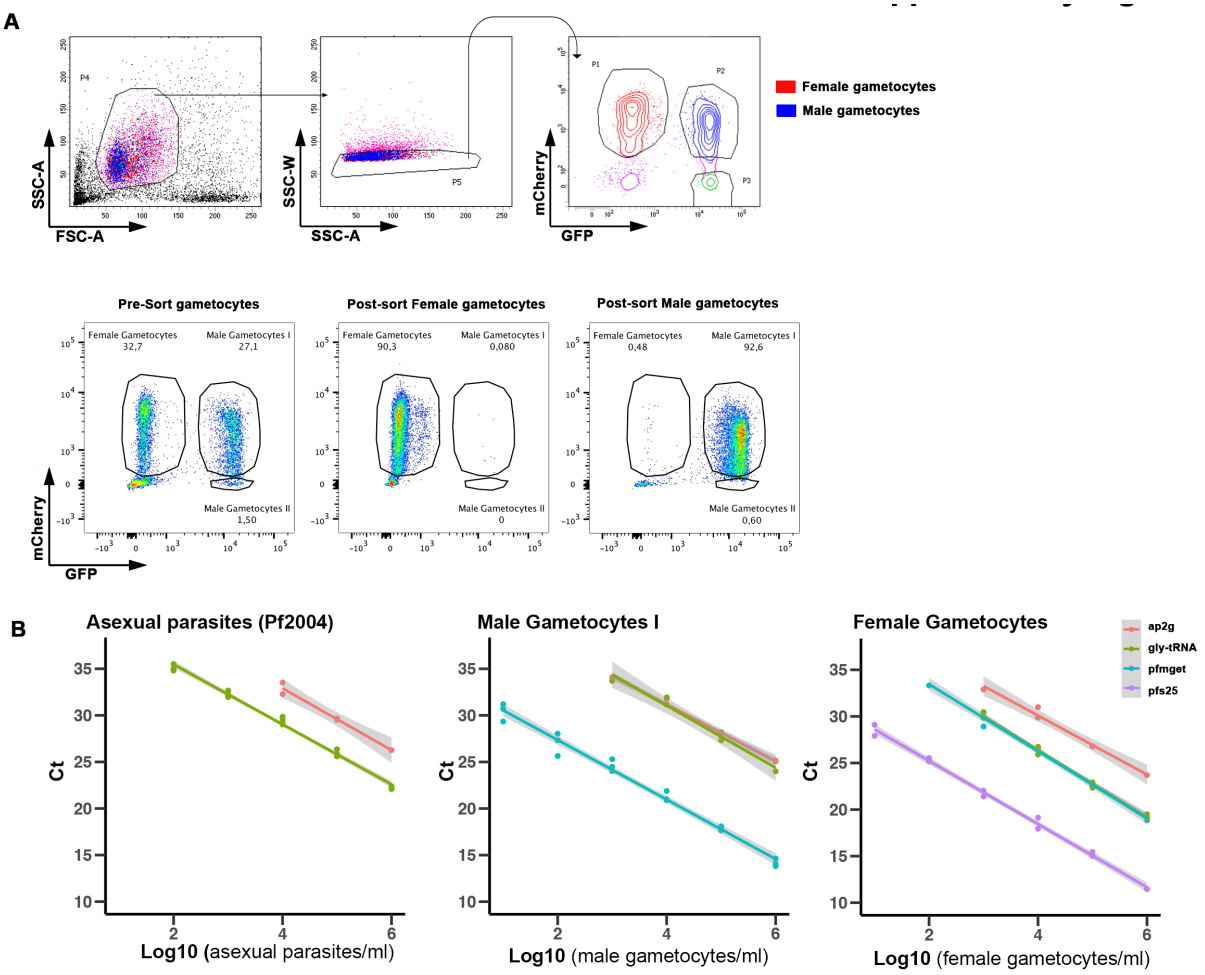

	pfs25	*gly-tRNA-lig*	*ap2g*	*pfmget*
Slope	-3.39	-3.242	-3.01	-3.193
Efficiency	97.42	103.63	114.9	106.09

Supplementary Figure 2

A Flow cytometry gating strategy to identify and sort PfDynGFP/ PfP47 gametocytes by mCherry and GFP expression into three populations (female: mCherry-positive, male I: mCherry- GFP-positive, male II: GFP-positive).**B** Pre-sort gametocyte distribution, and post-sorting purity verification of female and male gametocytes. **C** Serial dilutions of cDNA of asexual parasites and post-sort male and female gametocytes. Serial dilutions were used as standard curves to quantify total parasites, male and female gametocytes from q-RTPCR data of *pfs25*, *pfmget*, Glycine-tRNA ligase and to determine primer efficiency. Primer efficiency is shown on the figure. Primer efficiency of glycine-tRNA-ligase primers was determined based on asexual parasites, *pfs25* primer-efficiency based on female gametocytes and *ap2g* and *pfmget* in male gametocytes.

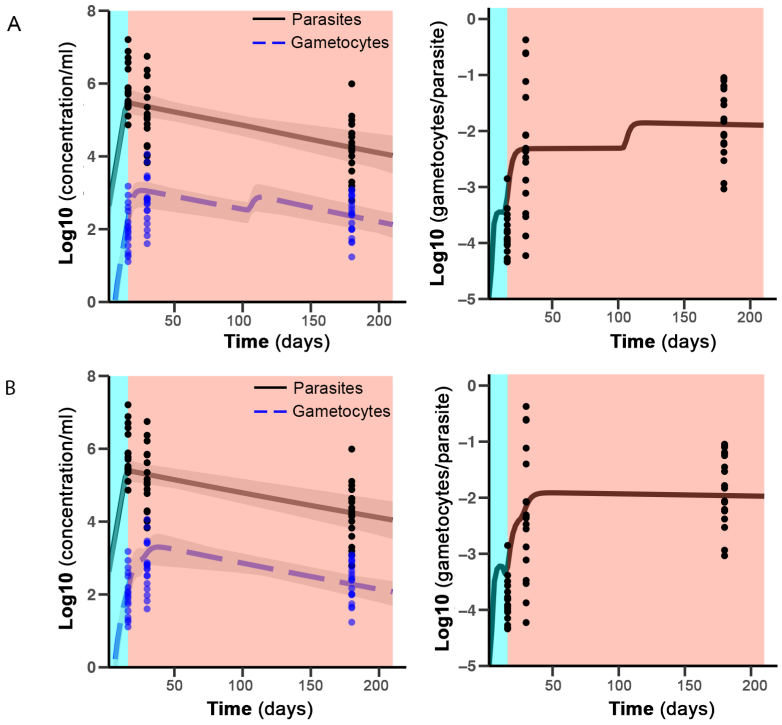

C

	Scenario 1		Scenario 2		Scenario 3	
Sexual Commitment Rate	0.11- 0.404 %		0.104 - 0.376%		0.193 - 0.896 %	
Modified Sex. Commitment Rate	NA		f2: 0.348 - 1.01 %		f3: 0.109 - 0.324 %	
Gametocyte Circulation time	1.9 - 2.4 days		1.3 - 1.9 days		1.2 -2.3 days	
Gametocyte Sequestration time	3.1 - 4.8 days		3.1 - 5.4 days		3.2 - 7.9 days	
	Acute Phase	Chronic Phase	Acute Phase	Chronic Phase	Acute Phase	Chronic Phase
Parasite multiplication factor	2.39 - 3.02	0.76 - 1.22	2.39 - 3.12	0.72 - 1.26 (f2: 0.72 - 1.26)	2.41 - 3.02 (f3: 2.4 - 3.02)	0.78 - 1.21 (f3: 0.78 - 1.22)

Supplementary Figure 3

A Model prediction of development of parasitemia and gametocytemia (left) and gametocyte/parasite ratio (right) with infection progression in scenario 2. Average prediction is shown, grey shaded indicate the minimum and maximum estimate of parasitemia and gametocytemia based on posterior parameter distribution. Parasitemia and gametocytemia are shown averaged over a cycle length (48 h). Lines indicate model prediction, measurements for gametocytemia of MAL (d14), Jan (d28) and May (d180) are shown. **B** Development of parasitemia, gametocytemia and gametocyte/parasite ratio in scenario 3. Parasitemia and gametocytemia are shown averaged over a cycle length (48 h). Lines indicate model prediction, measurements for gametocytemia of MAL (d14), Jan (d28) and May (d180) are shown. **C** Biological parameter estimates of *P. falciparum* infection shown as 89% credibility interval of the posterior distributions in the three modelled scenarios.

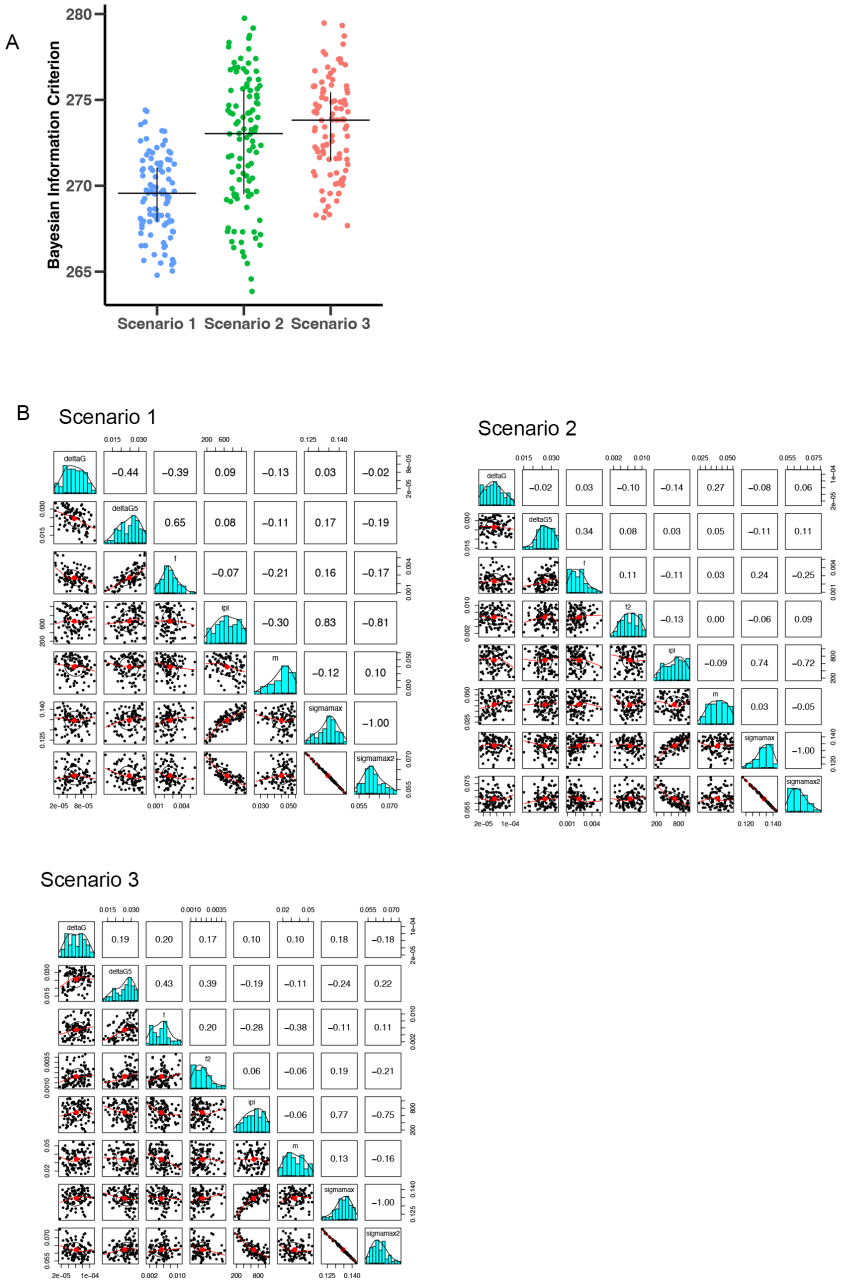

Supplementary Figure 4
A Bayesian information criterion for the three scenarios calculated based on the parameter estimates in the 10th pyABC generation after which the algorithm was stopped. **B** Correlation between parameter estimates in the final pyABC generation in the three scenarios. Posterior parameter distributions are shown on the diagonal, with the plots in the bottom triangular matrix showing scatterplots of each parameter combination, and numbers in the top triangular matrix indicating Pearson's correlation coefficient of individual parameter combinations.

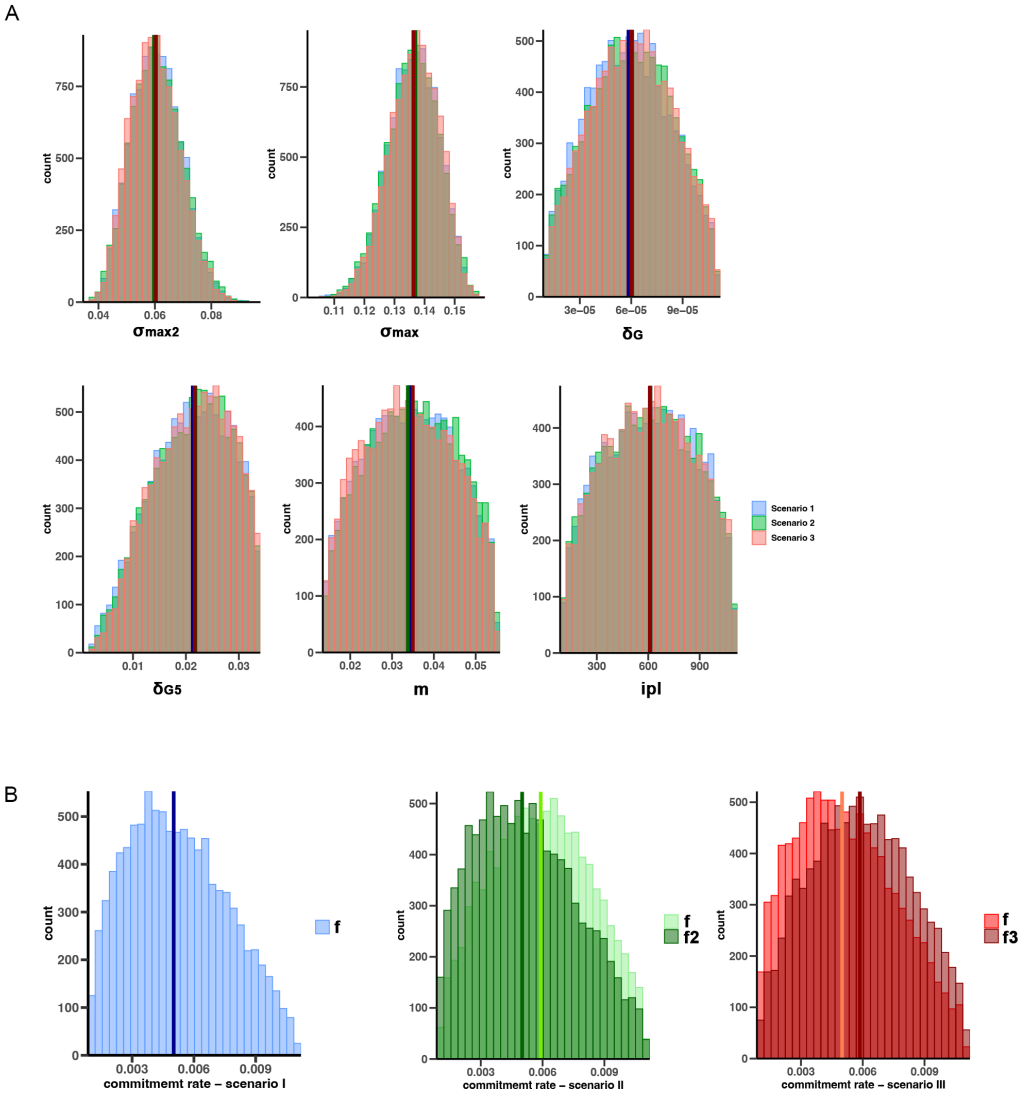

Supplementary Figure 5

A Posterior parameter distributions of the three model scenarios of all parameters except the commitment rate. Histogram of parameter estimates from 100 pyABC fitting runs with each evaluated after the 10th generation. Vertical lines indicate median parameter estimates. **B** Histogram of posterior distribution of the commitment rate in the three model scenarios, estimates from 100 pyABC fitting runs are shown with each evaluated after the 10th generation.

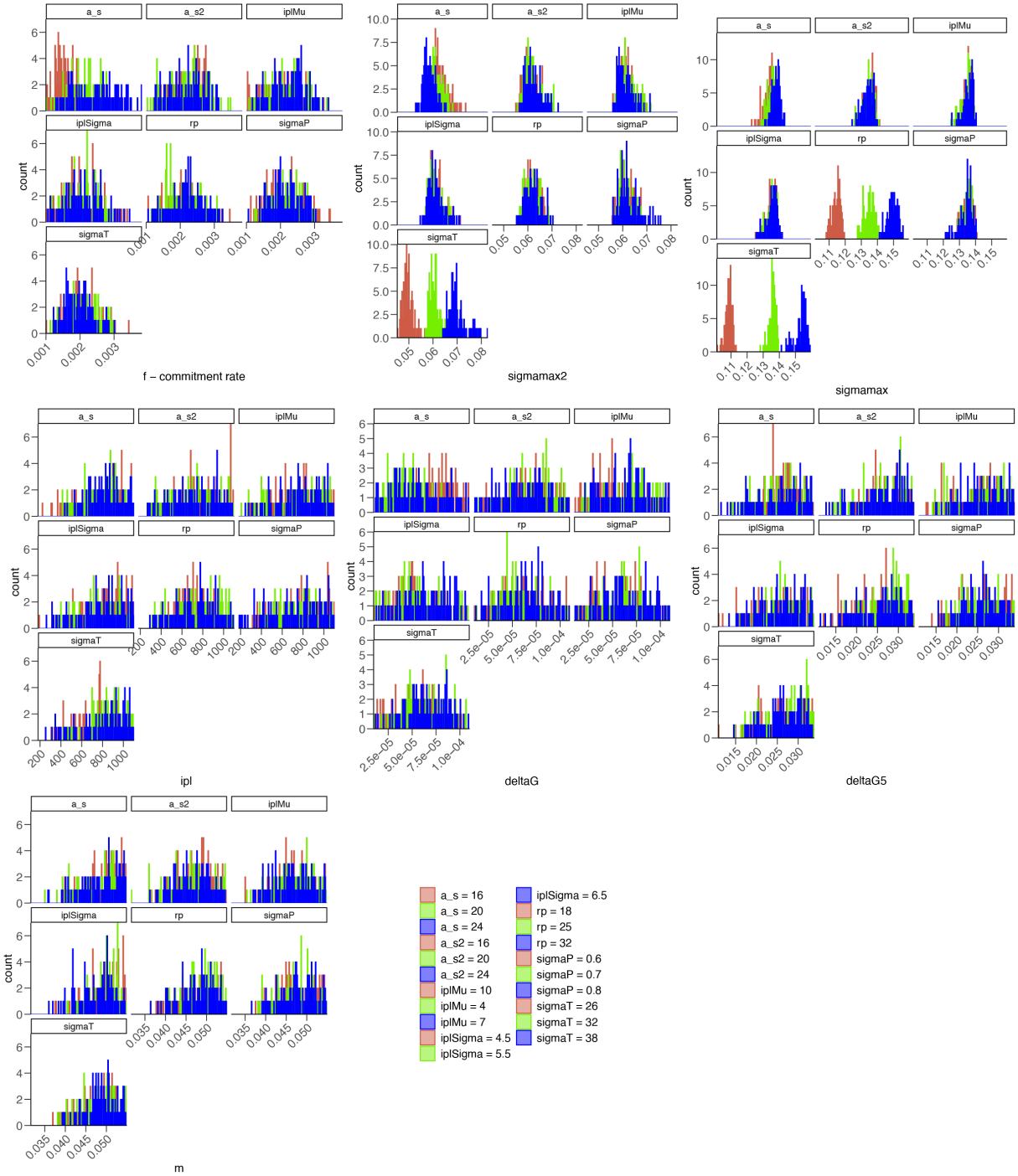

Supplementary Figure 6

Sensitivity analysis. Histograms of posterior parameter distribution of model parameters in scenario I in response to variation of model constant. Parameters were fitted to a model with a high (blue), middle (green) and low (red) parameter value for each model constant. Each set of plots corresponds to one model parameter, with each small plot showing posterior distribution under variations of one model constant.

1113